JOC Article

# Tandem Pseudopericyclic Reactions: [1,5]-X Sigmatropic Shift/ 6π-Electrocyclic Ring Closure Converting *N*-(2-X-Carbonyl)phenyl Ketenimines into 2-X-Quinolin-4(3*H*)-ones†

Mateo Alajarín,* María-Mar Ortín, Pilar Sánchez-Andrada,* and Ángel Vidal

*Departamento de Química Orgánica, Facultad de Química, Campus de Espinardo, Universidad de Murcia, 30100 Murcia, Spain*

*alajarin@um.es*

*Received June 22, 2006*

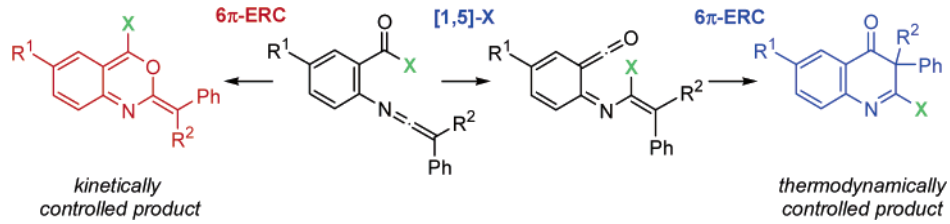


*N*-(2-X-Carbonyl)phenyl ketenimines undergo, under mild thermal conditions, [1,5]-migration of the X group from the carbonyl carbon to the electron-deficient central carbon atom of the ketenimine fragment, followed by a 6π-electrocyclic ring closure of the resulting ketene to provide 2-X-substituted quinolin-4(3*H*)-ones in a sequential one-pot manner. The X groups tested are electron-donor groups, such as alkylthio, arylthio, arylseleno, aryloxy, and amino. When involving alkylthio, arylthio, and arylseleno groups, the complete transformation takes place in refluxing toluene, whereas for aryloxy and amino groups the starting ketenimines must be heated at 230 °C in a sealed tube in the absence of solvent. The mechanism for the conversion of these ketenimines into quinolin-4(3*H*)-ones has been studied by ab initio and DFT calculations, using as model compounds *N*-(2-X-carbonyl)vinyl ketenimines bearing different X groups (X = F, Cl, OH, SH, $NH_2$, and $PH_2$) converting into 4(3*H*)-pyridones. This computational study afforded two general reaction pathways for the first step of the sequence, the [1,5]-X shift, depending on the nature of X. When X is F, Cl, OH, or SH, the migration occurs in a concerted mode, whereas when X is $NH_2$ or $PH_2$, it involves a two-step sequence. The order of migratory aptitudes of the X substituents at the acyl group is predicted to be $PH_2$ > Cl > SH > $NH_2$ > F> OH. The second step of the full transformation, the 6π-electrocyclic ring closure, is calculated to be concerted and with low energy barriers in all the cases. We have included in the calculations an alternative mode of cyclization of the *N*-(2-X-carbonyl)vinyl ketenimines, the 6π-electrocyclic ring closure leading to 1,3-oxazines that involves its 1-oxo-5-aza-1,3,5-hexatrienic system. Additionally, the pseudopericyclic topology of the transition states for some of the [1,5]-X migrations (X = F, Cl, OH, SH), for the 6π-electrocyclization of the ketene intermediates to the 4(3*H*)-pyridones, and for the 6π-electrocyclization of the starting ketenimines into 1,3-oxazines could be established on the basis of their geometries, natural bond orbital analyses, and magnetic properties. The calculations predict that the 4(3*H*)-pyridones are the thermodynamically controlled products and that the 1,3-oxazines should be the kinetically controlled ones.

## Introduction

Ketenimines are nitrogenated heterocumulenes [$R^1$-N=C=$CR^2R^3$] employed in organic synthesis mainly for the construction of nitrogen-containing heterocycles, via (1) the addition of nucleophiles[1] or radicals[2] to its central carbon atom; (2) the attack of electrophiles to its nitrogen atom, which also behaves as a donor atom in the formation of metallic σ complexes;[3] and (3) its participation in pericyclic events such as 6π-electrocyclic ring closures (ERC), cycloaddition reactions, and sigmatropic rearrangements.[1e] Among these reactions, sigmatropic rearrangements in ketenimines have received minor attention, and

† Dedicated to Prof. Marcial Moreno-Mañas in memoriam.

* Corresponding author. Phone: +34 968 367497. Fax: +34 968 364149.

10.1021/jo061286e CCC: $33.50 
Published on Web 09/19/2006

they have been scarcely reported. Some examples of [3,3]-, [1,3]- and [1,5]-sigmatropic migrations in ketenimines have been reported; in most of them the migrating group reaches the central carbon atom of the ketenimine.

Concerning the [3,3]-sigmatropic migration, Brannock and Burpitt,[4] in a seminal paper in 1965, reported the conversion of *N*-(2-alkenyl)amides into 4-pentenenitriles by the phosphorus pentachloride/triethylamine combination of reagents. They postulated *N*-(2-alkenyl) ketenimines as reaction intermediates, suggesting that these species undergo a 3-aza-Claisen rearrangement to the unsaturated nitriles. Afterward, Walters[5] and some of us[6] carried out an extensive investigation of this [3,3]-rearrangement in a variety of new 2-(alkenyl) ketenimines, which included the development of new methods for the synthesis of this type of ketenimines, an experimental study of the stereocontrol of this reaction, and a computational study of the 3-aza-Claisen rearrangement of 3-aza-1,2,5-hexatrienes. This thermally induced 3-aza-Claisen rearrangement of *N*-(2-alkenyl) ketenimines has been used as a key step in efficient asymmetric syntheses of the chiral natural products (+)-canadensolide, (+)-santolinolide B, and (−)-santolinolide A.[7]

The more important research works dealing with [1,3]-sigmatropic shifts in ketenimines have been reported by Wentrup,[8a−h] who carried out an extensive study of the reversible *C*-acyl ketenimine to imidoyl ketene rearrangement, via [1,3]-sigmatropic shifts of a variety of atoms or groups of atoms under flash vacuum pyrolysis (FVP) conditions. In these processes,

**SCHEME 1. [1,3]-Sigmatropic Shifts in *C*-Acyl Ketenimines**

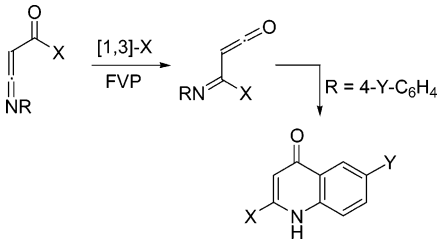


**CHART 1. *N*-(2-X-Carbonyl)phenyl Ketenimines**

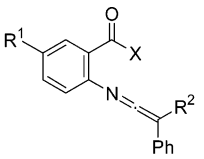


X = $SR^3$, SeAr, OAr, $NR^3R^4$, Br, Cl

when (*N*-aryl)imidoyl ketenes are formed they underwent further 6$\pi$-electrocyclization to quinolin-4(1*H*)-ones (Scheme 1).[8b,d−f,9]

To our knowledge, only three examples of [1,5]-sigmatropic shifts in ketenimines have been described so far, and all of them involve a [1,5]-hydrogen atom transfer to the central carbon of the ketenimine. Goerdeler[10] reported that *C*-imidoyl ketenimines underwent, at room temperature, a [1,5]-H shift followed by ERC to yield dihydropyrimidines. On the other hand, Foucaud[11] demonstrated that in refluxing dichloromethane *N*-imidoyl ketenimines converted into pyrrolotriazines by a consecutive [1,5]-H shift/intramolecular [4 + 2]-cycloaddition. More recently, Wentrup[12] published that *N*-aryl ketenimines bearing methyl groups at the ortho position suffer, under flash vacuum thermolysis conditions, a facile [1,5]-H shift and subsequent electrocyclization to dihydroquinolines.

In the frame of a systematic development of new reactions of ketenimines, we targeted the synthesis of a variety of *N*-(2-X-carbonyl)phenyl ketenimines (Chart 1), with the aim of examining the viability of the [1,5]-migration of diverse X groups from the carbonyl carbon to the electron-deficient central carbon atom of the ketenimine fragment. We focused on testing the sigmatropic migration of electron-donor groups, such as alkylthio, arylthio, arylseleno, aryloxy, amino, and halides, given the electrophilic character of the presumed migration terminus.

In this paper, we report that in fact such ketenimines undergo a facile [1,5]-sigmatropic migration of the X group under mild thermal conditions and a subsequent 6$\pi$-electrocyclic ring closure of the resulting ketene to afford 2-X-substituted quinolin-4(3*H*)-ones. Furthermore, we have carried out a computational study in order to gain insight on the mechanism of these transformations and to evaluate the relative migratory aptitude of the different X groups. In a previous communication, we have reported that *N*-[2-(alkyl- or arylthio)carbonyl]phenyl ketenimines undergo cyclization to afford 2-alkyl(aryl)thio-

(1) For reviews on the chemistry of ketenimines, see: (a) Krow, D. R. *Angew. Chem., Int. Ed. Engl.* **1971**, *10*, 435−449. (b) Gambaryan, N. P. *Usp. Khim.* **1976**, *45*, 1251−1268. (c) Dondoni, A. *Heterocycles* **1980**, *14*, 1547−1566. (d) Barker, M. W.; McHenry, W. E. In *The Chemistry of Ketenes, Allenes and Related Compounds*; Patai, S., Ed.; Wiley-Interscience: Chichester, U.K., 1980; Part 2, p 701. (e) Alajarín, M.; Vidal, A.; Tovar, F. *Targets Heterocycl. Syst.* **2000**, *4*, 293−326.

(2) (a) Alajarín, M.; Vidal, A.; Ortín, M.-M. *Tetrahedron Lett.* **2003**, *44*, 3027−3030. (b) Alajarín, M.; Vidal, A.; Ortín, M.-M. *Org. Biomol. Chem.* **2003**, *1*, 4282−4292. (c) Alajarín, M.; Vidal, A.; Ortín, M.-M.; Bautista, D. *New J. Chem.* **2004**, *28*, 570−577. (d) Alajarín, M.; Vidal, A.; Ortín, M.-M.; Bautista, D. *Synlett* **2004**, 991−994.

(3) (a) Aumann, R. *Chem. Ber.* **1993**, *126*, 1867−1872. (b) Merlic, C. A.; Burns, E. E. *Tetrahedron Lett.* **1993**, *34*, 5401−5404.

(4) Brannock, K. C.; Burpitt, R. D. *J. Org. Chem.* **1965**, *30*, 2564−2565.

(5) (a) Walters, M. A.; McDonough, C. S.; Brown, P. S., Jr.; Hoem, A. B. *Tetrahedron Lett.* **1991**, *32*, 179−182. (b) Walters, M. A.; Hoem, A. B.; Arcand, H. R.; Hegeman, A. D.; McDonough, C. S. *Tetrahedron Lett.* **1993**, *34*, 1453−1456. (c) Walters, M. A.; Hoem, A. B. *J. Org. Chem.* **1994**, *59*, 2645−2647. (d) Walters, M. A. *J. Am. Chem. Soc.* **1994**, *116*, 11618−11619. (e) Walters, M. A. *J. Org. Chem.* **1996**, *61*, 978−983.

(6) (a) Molina, P.; Alajarín, M.; López-Leonardo, C. *Tetrahedron Lett.* **1991**, *32*, 4041−4044. (b) Molina, P.; Alajarín, M.; López-Leonardo, C.; Alcántara, J. *Tetrahedron* **1993**, *49*, 5153−5168.

(7) Nubbemeyer, U. *Synthesis* **1993**, 1120−1128.

(8) (a) Cheikh, A. B.; Chuche, J.; Manisse, N.; Pommelet, J. C.; Netsch, K.-P.; Lorencak, P.; Wentrup, C. *J. Org. Chem.* **1991**, *56*, 970−975. (b) Kappe, C. O.; Kollenz, G.; Leung-Toung, R.; Wentrup, C. *J. Chem. Soc., Chem. Commun.* **1992**, 487−488. (c) Kappe, C. O.; Kollenz, G.; Netsch, K.-P.; Leung-Toung, R.; Wentrup, C. *J. Chem. Soc., Chem. Commun.* **1992**, 488−490. (d) Fulloon, B.; El-Nabi, H. A. A.; Kollenz, G.; Wentrup, C. *Tetrahedron Lett.* **1995**, *36*, 6547−6550. (e) Fulloon, B. E.; Wentrup, C. *J. Org. Chem.* **1996**, *61*, 1363−1368. (f) Ramana Rao, V. V.; Wentrup, C. *J. Chem. Soc., Perkin Trans. 1* **1998**, 2583−2586. (g) Wentrup, C.; Ramana Rao, V. V.; Frank, W.; Fulloon, B. E.; Moloney, D. W. J.; Mosandl, T. *J. Org. Chem.* **1999**, *64*, 3608−3619. (h) Finnerty, J. J.; Wentrup, C. *J. Org. Chem.* **2004**, *69*, 1909−1918. For other papers dealing with [1,3]-migration in ketenimines, see: (i) Aumann, R.; Heinen, H. *Chem. Ber.* **1988**, *121*, 1739−1743. (j) Clarke, D.; Mares, R. W.; McNab, H. *J. Chem. Soc., Chem. Commun* **1993**, 1026−1027. (k) Clarke, D.; Mares, R. W.; McNab, H. *J. Chem. Soc., Perkin Trans. 1* **1997**, 1799−1804. (l) Amsallem, D.; Mazières, S.; Piquet-Fauré, V.; Gornitzka, H.; Baceiredo, A.; Bertrand, G. *Chem.-Eur. J.* **2002**, *8*, 5306−5311.

(9) The Conrad−Limpach synthesis of quinolones by pyrolysis of esters probably proceeds via imidoyl ketene intermediates: Conrad, M.; Limpach, L. *Ber. Dtsch. Chem. Ges.* **1887**, *20*, 944−948. The first report on the observation of imidoyl ketenes in quinolone synthesis: Briehl, H.; Adelheid, L.; Wentrup, C. *J. Org. Chem.* **1984**, *49*, 2772−2779.

(10) Goerdeler, J.; Lindner, C.; Zander, F. *Chem. Ber.* **1981**, *114*, 536−548.

(11) Morel, G.; Marchand, E.; Foucaud, A. *J. Org. Chem.* **1985**, *50*, 771−778.

(12) Ramana Rao, V. V.; Fulloon, B. E.; Bernhardt, P. V.; Koch, R.; Wentrup, C. *J. Org. Chem.* **1998**, *63*, 5779−5786.

**SCHEME 2. Synthesis of Quinolin-4(3*H*)-ones 5**[a]

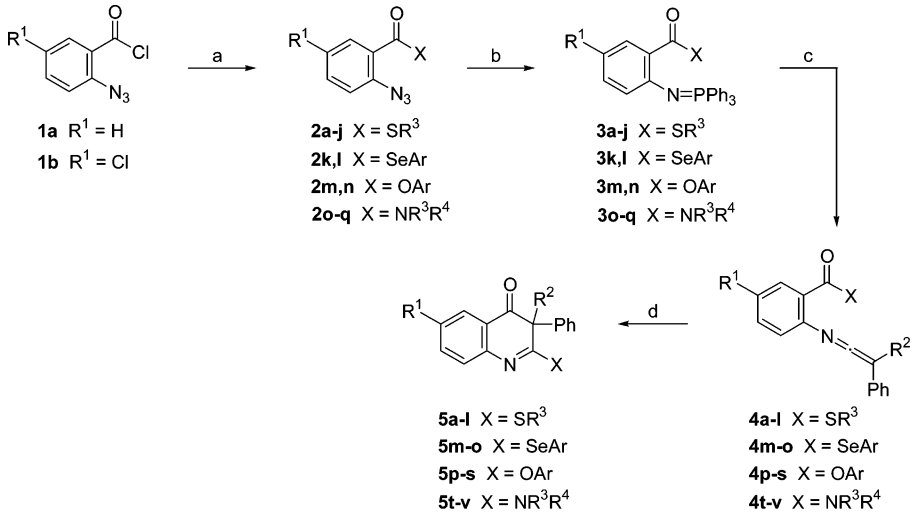


[a] Reagents and conditions: (a) For X = $SR^3$: $R^3SH$, DMAP, $CH_2Cl_2$, rt, 5 h. For X = SeAr: ArSeSeAr, $NaBH_4$, EtOH, rt, 3 h. For X = OAr: ArOH, DMAP, $CH_2Cl_2$, rt, 5 h. For X = $NR^3R^4$: $R^3R^4NH$, pyridine, 0 °C, 1.5 h. (b) For X = $SR^3$, OAr, $NR^3R^4$: $PPh_3$, $Et_2O$, rt, 16 h. For X = SeAr: $PPh_3$, toluene, rt, 4 h. (c) For X = $SR^3$, SeAr: $PhR^2C{=}C{=}O$, toluene, rt, 15 min. For X = OAr, $NR^3R^4$: $PhR^2C{=}C{=}O$, $CH_2Cl_2$, rt, 15 min. (d) For X = $SR^3$, SeAr: toluene, reflux, 1 h. For X = OAr, $NR^3R^4$: neat, sealed tube, 230 °C, 1 h.

quinolin-4(3*H*)-ones by means of a consecutive 1,5-migration of the alkyl(aryl)thio group/6$\pi$-electrocyclization.[13]

## Results and Discussion

**Experimental Study.** First, we tested the migration of alkyl(aryl)thio groups in *N*-[2-alkyl(aryl)thiocarbonyl]phenyl ketenimines **4a**−**l**.[14] The reaction of 2-azidobenzoyl chloride **1a** and 2-azido-5-chlorobenzoyl chloride **1b** with alkylthiols and arylthiols, in dichloromethane solution, in the presence of a slight excess of DMAP, afforded the *S*-alkyl and *S*-aryl 2-azidothiobenzoates **2a**−**j**. The treatment of the 2-azidothiobenzoates **2a**−**j**, in diethyl ether solution, with triphenylphosphine provided the 2-(triphenylphosphoranylideneamino)thiobenzoates **3a**−**j**. The reaction of triphenylphosphazene **3a** ($R^1$ = H; X = 4-$CH_3C_6H_4S$), in dichloromethane solution at room temperature, with a stoichiometric amount of diphenylketene gave ketenimine **4a** ($R^1$ = H; X = 4-$CH_3C_6H_4S$; $R^2$ = Ph), which was purified by column chromatography on silica gel, isolated, and fully identified.[14] When a toluene solution of **4a** was heated at reflux temperature for approximately 1 h, an IR spectra of the reaction mixture showed the total disappearance of the cumulenic band around 2000 $cm^{-1}$ associated with the N=C=C grouping, and from the resulting crude material 2-(4-methylphenylthio)-3,3-diphenylquinolin-4(3*H*)-one **5a** ($R^1$ = H; X = 4-$CH_3C_6H_4S$; $R^2$ = Ph) was isolated by column chromatography as the only reaction product (Scheme 2).

Following this initial experiment, the aza-Wittig reactions of a series of organosulfur iminophosphoranes **3a**−**j** with diphenylketene and methylphenylketene were carried out in toluene solution, at room temperature, to give the corresponding ketenimines **4a**−**l**, whose formation was confirmed by IR spectra of the reaction mixtures. The heating of toluene solutions containing ketenimines **4a**−**l** at reflux temperature for 1 h provided the respective 2-alkyl(aryl)thioquinolin-4(3*H*)-ones **5a**−**l** in acceptable yields (Scheme 2, Table 1). The conversions **4a**−**l** → **5a**−**l** also took place at room temperature, although most of these reactions required up to 48 h to be completed. The structural determination of the 2-alkyl(aryl)thioquinolin-4(3*H*)-ones **5a**−**l** was achieved following their analytical and spectral data and was unequivocally established by the X-ray structure determination of a monocrystal of **5a** ($R^1$ = H; X = 4-$CH_3C_6H_4S$; $R^2$ = Ph).[14]

**TABLE 1. Quinolin-4(3*H*)-ones 5**

| compd | $R^1$ | X | $R^2$ | yield (%) |
|---|---|---|---|---|
| **5a** | H | 4-$CH_3C_6H_4S$ | Ph | 74 |
| **5b** | H | 4-$CH_3C_6H_4S$ | Me | 52 |
| **5c** | H | 4-$CH_3OC_6H_4S$ | Ph | 89 |
| **5d** | H | 4-($C_5H_5N$)S | Ph | 79 |
| **5e** | Cl | 4-$CH_3C_6H_4S$ | Ph | 97 |
| **5f** | Cl | 4-$CH_3OC_6H_4S$ | Ph | 95 |
| **5g** | Cl | 4-$CH_3OC_6H_4S$ | Me | 76 |
| **5h** | H | 4-$CH_3OC_6H_4CH_2S$ | Ph | 83 |
| **5i** | H | $C_6H_5(CH_3)CHS$ | Me | 58[a] |
| **5j** | Cl | 4-$CH_3OC_6H_4CH_2S$ | Ph | 51 |
| **5k** | H | $C_6H_5CH_2CH_2S$ | Ph | 85 |
| **5l** | H | 2-$IC_6H_4CH_2CH_2S$ | Ph | 90 |
| **5m** | H | $C_6H_5Se$ | Ph | 62 |
| **5n** | H | $C_6H_5Se$ | Me | 60 |
| **5o** | H | 4-$CH_3OC_6H_4Se$ | Ph | 36 |
| **5p** | H | 4-$CH_3C_6H_4O$ | Ph | 42 |
| **5q** | H | 4-$CH_3C_6H_4O$ | Me | 28 |
| **5r** | H | 3,4-$(CH_3O)_2C_6H_3O$ | Ph | 36 |
| **5s** | H | 3,4-$(CH_3O)_2C_6H_3O$ | Me | 25 |
| **5t** | H | $(CH_3)_2N$ | Ph | 36 |
| **5u** | H | $C_6H_5(CH_3)N$ | Ph | 30 |
| **5v** | H | $(4\text{-}CH_3C_6H_4)_2N$ | Ph | 25 |

[a] Isolated as a 1:1 mixture of two diastereoisomers.

Next, we prepared *N*-(2-arylselenocarbonyl)phenyl ketenimines **4m**−**o** from the *Se*-aryl 2-azidoselenobenzoates **2k,l** via a simple chemical sequence. Thus, treatment of solutions of diphenyl diselenide and bis(4-methoxyphenyl) diselenide, in anhydrous ethanol, with sodium borohydride provided sodium benzeneselenolate and 4-methoxybenzeneselenolate, which reacted with 2-azidobenzoyl chloride **1a**, leading to the respective

(13) Alajarín, M.; Ortín, M.-M.; Sánchez-Andrada, P.; Vidal, A.; Bautista, D. *Org. Lett.* **2005**, *7*, 5281−5284.

(14) The experimental work related with the [1,5]-migration of alkyl(aryl)thio groups in *N*-[2-alkyl(aryl)thiocarbonyl]phenyl ketenimines has been reported in our preliminary communication, ref 13.

formation of *Se*-phenyl 2-azidoselenobenzoate **2k** ($R^1$ = H; X = $C_6H_5Se$) and *Se*-(4-methoxyphenyl) 2-azidoselenobenzoate **2l** ($R^1$ = H; X = 4-$CH_3OC_6H_4Se$), in very low yields, whereas the major product isolated from these reactions was ethyl 2-azidobenzoate.[15] The sequential treatment at room temperature, and in the same reaction flask, of toluene solutions of the 2-azidoselenobenzoates **2k,l** with triphenylphosphine and diphenylketene or methylphenylketene led to the corresponding ketenimines **4m**−**o**, which converted into the respective 2-arylselenoquinolin-4(3*H*)-ones **5m**−**o** when their toluene solutions were heated at reflux temperature for 1 h (Scheme 2, Table 1).

The reaction of 2-azidobenzoyl chloride **1a** with 4-methylphenol and 3,4-dimethoxyphenol, in dichloromethane solution in the presence of DMAP, and the subsequent Staudinger reaction of the aryl 2-azidobenzoates **2m,n** with triphenylphosphine, in diethyl ether, provided in a straightforward manner the aryl 2-(triphenylphosphoranylideneamino)benzoates **3m,n**. Our first try at the [1,5]-migration of aryloxy groups in *N*-(2-aryloxycarbonyl)phenyl ketenimines was carried out by heating in either refluxing toluene or *o*-xylene solutions of the *C*,*C*-diphenyl ketenimine **4p** ($R^1$ = H; X = 4-$CH_3C_6H_4O$; $R^2$ = Ph), generated by reaction of compound **3m** ($R^1$ = H; X = 4-$CH_3C_6H_4O$) with diphenylketene in these solvents. We could establish that after 48 h under both reaction conditions compound **4p** remained unaltered, and the same result was obtained when **4p** was heated for the same time at 180 °C in toluene solution in a sealed tube. Afterward, ketenimine **4p** was generated in dichloromethane and, after removing the solvent, the mixture containing this ketenimine and the triphenylphosphine oxide was heated at 230 °C in a sealed tube up to the total disappearance of the cumulenic band in its IR spectrum, approximately 1 h. The material obtained from this thermal treatment was chromatographed, thus resulting in the isolation of pure 2-(4-methylphenyloxy)-3,3-diphenylquinolin-4(3*H*)-one **5p**, in 42% yield. The application of this procedure to the *N*-(2-aryloxycarbonyl)phenyl ketenimines **4q**−**s** yielded the corresponding 2-aryloxyquinolin-4(3*H*)-ones **5q**−**s** in low yields (Scheme 2, Table 1).

Finally, we were also able to achieve the [1,5]-shift of amino groups in *N*-(2-carbamoyl)phenyl ketenimines. The acylation of dialkyl, alkylaryl, or diaryl substituted secondary amines with 2-azidobenzoyl chloride **1a** led to the 2-azidobenzamides **2o**−**q**, which by the habitual methodology were converted into their respective *N*-(2-carbamoyl)phenyl ketenimines **4t**−**v**. We could convert ketenimines **4t**−**v** into the 2-aminoquinolin-4(3*H*)-ones **5t**−**v** only when these heterocumulenes were heated at 230 °C in a sealed tube in the absence of solvent, although the yields of these transformations were also low (Scheme 2, Table 1).

At this point of the discussion, it is worth mentioning that although we planned to test the migration of bromine and chlorine atoms in the *N*-(2-bromocarbonyl)phenyl ketenimine **4w** and the *N*-(2-chlorocarbonyl)phenyl ketenimine **4x**, respectively (Chart 2), unfortunately the strategies that we attempted for the preparation of these two ketenimines failed. These synthetic approaches involved either the use of starting materials bearing an acyl halide function or the generation of this function in the last step, in the presence of the ketenimine grouping.

**CHART 2. *N*-(2-Bromocarbonyl)phenyl Ketenimine 4w and *N*-(2-Chlorocarbonyl)phenyl Ketenimine 4x**

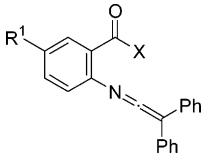


**4w** X = Br
**4x** X = Cl

**SCHEME 3. Proposed Mechanism for the Conversion 4→5**

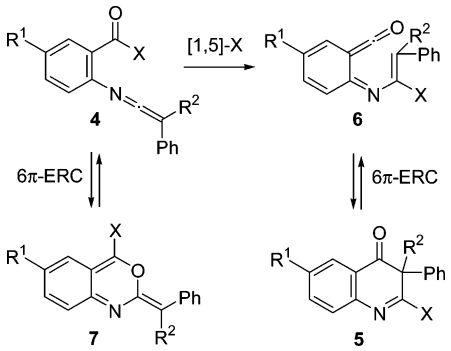


We assume that the mechanism of the transformation of the ketenimines **4** into the quinolin-4(3*H*)-ones **5** is initiated by the [1,5]-migration of the X group from the carbonyl carbon to the central carbon atom of the ketenimine moiety to give the imidoyl ketenes **6**, which are further converted into the reaction products **5** through a 6$\pi$-electrocyclic ring closure of their conjugated 3-azahexatriene fragment (Scheme 3). It is also conceivable that the *N*-(2-X-carbonyl)phenyl ketenimines **4** may experience cyclization to the 3,1-benzoxazines **7** via a 6$\pi$-electrocyclization involving their conjugated 1-oxa-5-azahexatrienic system. However, it does not seem to be the case, as compounds **7** were never detected in the $^1$H NMR spectra of the crude materials obtained from the thermal treatment of ketenimines **4**. Given that all the reactions in Scheme 3 can be chemical equilibria, the exclusive formation of quinolin-4(3*H*)-ones **5** in the thermal treatment of ketenimines **4** may be a consequence of prevailing thermodynamic versus kinetic control. At first sight, compounds **5** seem more stable, on thermodynamic grounds, than the *o*-quinonoid benzoxazines **7**. This matter will be treated in depth in the following sections.

**Computational Study.** For simplicity, to model the transformation of the ketenimines **4** into the quinolin-4(3*H*)-ones **5** presented in the experimental part of this work, we selected the more simple structures **8c**−**e**, where the vinyl group joining the acyl and ketenimine functions models the benzene ring of the ketenimines **4** and the OH, SH, and $NH_2$ groups model the OAr, $SR^3$, and $NR^3R^4$ groups. In our previous communication,[13] we have shown computationally that the transformation of ketenimine **8d** (X = SH) into 2-thiohydroxy-4(3*H*)-pyridone **9d** occurs by a two-step pathway that starts with the [1,5]-shift in the SH group leading to an intermediate imidoyl ketene **10d**, which in a second step undergoes an electrocyclic ring closure

(15) We did not succeed in the synthesis of the *Se*-aryl 2-azidoselenobenzoates **2k,l** by using other well-established reaction conditions for the preparation of selenoesters, such as those used in the following articles: (a) Grieco, P. A.; Jaw, J. Y. *J. Org. Chem.* **1981**, *46*, 1215−1217. (b) Nicolaou, K. C.; Petasis, N. A.; Claremon, D. A. *Tetrahedron* **1985**, *41*, 4835−4841. (c) Gais, H.-J. *Angew. Chem., Int. Ed. Engl.* **1977**, *16*, 244−246. (d) Ireland, R. E.; Norbeck, D. W.; Mandel, G. S.; Mandel, N. S. *J. Am. Chem. Soc.* **1985**, *107*, 3285−3294. Probably the *o*-azido group of **1** interferes with the expected substitution at the acyl group. Only a modification of the experimental procedure described by Odom for the preparation of selenoesters from acyl chlorides and benzeneselenolates, generated by reaction of diaryl diselenides and sodium borohydride, provided the *Se*-aryl 2-azidoselenobenzoates **2k**,**l**, although in very low yields, see: (e) Mullen, G. P.; Luthra, N. P.; Dunlap, R. B.; Odom, J. D. *J. Org. Chem.* **1985**, *50*, 811−816.

**SCHEME 4. Intramolecular Cyclization Modes for the Ketenimines 8a−f**

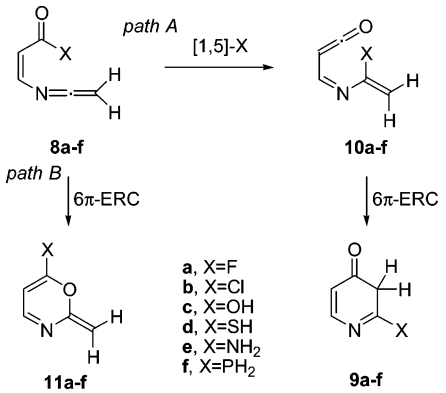


to provide the 4(3*H*)-pyridone **9d**. In this mechanistic scheme the rate-determining step was the [1,5]-sigmatropic rearrangement of the SH group. To gain insight on the migrating aptitudes of the different X groups and a deeper understanding of the mechanistic aspects of this process, we have considered in this study, besides the migrating groups above-mentioned, the fluorine and chlorine atoms and the $PH_2$ group, by including them on the ketenimines **8a**, **8b**, and **8f**, respectively.

We have explored the potential energy surface associated with the transformation of the ketenimines **8a**−**f** into the 4(3*H*)-pyridones **9a**−**f** (Scheme 4, path A). On the other hand, the 1-oxo-5-aza-1,3,5-hexatrienic system present in ketenimimes **8** enables these compounds to experience a 6$\pi$-electrocyclic ring closure, leading to the 2-methylene-6-substituted-1,3-oxazines **11** (path B). Due to its presumable pseudopericyclic nature, this process is expected to occur easily,[16] and consequently it could compete with path A. This is the reason we have also included in our calculations this alternative mode of cyclization of the ketenimines **8**.

It is worth emphasizing from the beginning of this discussion that the structural characteristics of the ketenimines **8a**−**f** and the ketene intermediates **10a**−**f** open the possibility that the [1,5]-sigmatropic rearrangements and the two 6$\pi$-electrocyclic ring closures delineated in Scheme 4 (**8a**−**f**→**11a**−**f** and **10a**−**f**→**9a**−**f**) can take place in a pseudopericyclic way. Note that in the three reactions in that scheme a more or less nucleophilic atom becomes linked to the central carbon of a heterocumulene function. Thus, with the aim of knowing the precise nature of these transformations, in this computational study we have paid special attention to the characterization of the orbital topology of their respective transition states.

Figures 1 and 4 display the qualitative reaction profiles at the B3LYP/6-31+G* theoretical level and the location of the stationary points for the transformation of ketenimines **8a**−**f** into **9a**−**f** and **11a**−**f**. Figures 2, 3, and 5−7 show the geometries of the transition states **TS1a**−**d**, **TS2a**−**d**, and **TS3a**−**f** and the stationary points found in the transformations **8e**,**f**→**9e**,**f**/**11e**,**f**, including relevant bond distances. Table 2 includes the relative energies of the stationary points at the B3LYP/6-31+G*//B3LYP/6-31+G* theoretical level and the energy barriers. Zero-point vibrational energy corrections have been applied, but not scaled. We will comment only on the results obtained at the B3LYP/6-31+G* theoretical level, unless otherwise stated.

**Path A. Transformation of Ketenimines 8a−f into the 4(3*H*)-Pyridones 9a−f.** Surprisingly, depending on the nature of the migrating group X, we have found two different general pathways for the conversion of ketenimines **8a**−**f** into the 4(3*H*)-pyridones **9a**−**f**. Thus, when X is F, Cl, OH, or SH (**8a**−**d**), the [1,5]-X shift occurs in a concerted mode, whereas when X is $NH_2$ or $PH_2$ (**8e** and **8f**) the migration of the $NH_2$ or the $PH_2$ group involves a two-step mechanistic scheme. We next discuss separately these two reaction pathways, concerted and stepwise.

**Concerted [1,5]-X Sigmatropic Rearrangement of Ketenimines 8a−d to Ketenes 10a−d and Subsequent 6$\pi$-Electrocyclic Ring Closure Leading to 4(3*H*)-Pyridones 9a−d.** The intensive search along both HF/6-31G* and B3LYP/6-31+G* potential energy surfaces revealed a similar mechanism for the transformation of the four ketenimines **8a**−**d** (X = F, Cl, OH, and SH) into their respective 4(3*H*)-pyridones **9a**−**d**. The first step consists of a [1,5]-shift of the X group, via the transition structures **TS1a**−**d** (Figure 2), leading to the intermediate ketenes **10a**−**d**, which in a second step undergo an electrocyclic ring closure, through the transition states **TS2a**−**d**, to give the final 4(3*H*)-pyridones **9a**−**d**.

The computed energy barriers for the first step, the [1,5]-X shift, range from 22.90 (X = OH) to 15.76 (X = Cl) kcal·mol$^{-1}$, the process being slightly endothermic (by 3.56−10.23 kcal·mol$^{-1}$). The energy barrier for the prototypical [1,5]-H shift in *cis*-1,3-pentadiene, which has been calculated to be 32.6 kcal·mol$^{-1}$ from the *s*-cis conformer,[17] is significantly higher than those corresponding to the present [1,5]-X shifts converting the ketenimines **8a**−**d** into the ketenes **10a**−**d**. The geometries of the transition states **TS1a**−**d** are planar or nearly planar. In contrast, the transition structure of the suprafacial [1,5]-H shift in 1,3-pentadiene (**TS1ref**, see Supporting Information) resembles a slightly flattened cyclohexane ring,[18] the migrating hydrogen projecting out of the plane and the HCCC dihedral angle being 27.6°. The molecular skeletons of **TS1a** and **TS1b** are essentially planar, the F and Cl atoms migrating in the molecular plane (see the values of the dihedral angles in Figure 2), where the LUMO of the ketenimine moiety is placed. The situation is similar in **TS1c** (X = OH), but in this case, the OH group projects slightly out the plane. In **TS1d** (X = SH) the molecular skeleton deviates more notably from planarity and the values of the SC1N3C4 and SC6C5C4 dihedral angles are 28.9° and 18.0° respectively.

The computed energy barriers for the second step in the cyclization **8a**−**d**→**9a**−**d**, that is, the 6$\pi$-electrocyclic ring closure of **10a**−**d** to **9a**−**d**, are very low, ranging from 1.51 to 5.20 kcal·mol$^{-1}$, and in all the cases the process is exothermic. By comparing the values of the barriers associated with these ring closures with that calculated for the archetypical 6$\pi$-electrocyclic ring closure of 1,3,5-hexatriene to 1,3-cyclohexadiene, which has been computed to be 26.6 kcal mol$^{-1}$,[19] it is clear that the barriers for the cyclization of ketenes **10a**−**d** to

(16) We have reported that a similar ring closure transforming *N*-$\beta$-(methyleneaminoacyl)vinyl ketenimine into 6-methyleneamino-2-methylene-1,3-oxazine takes place trough a transition state of pseudopericyclic topology and low energy barrier; see: Alajarín, M.; Sánchez−Andrada, P.; Vidal, A.; Tovar, F. *J. Org. Chem.* **2005**, 70, 1340−1349.

(17) (a) Saettel, N. J.; Wiest, O. *J. Org. Chem.* **2000**, *65*, 2331−2336. (b) Hess, B. A.; Baldwin, J. E. *J. Org.* Chem. **2002**, *67*, 6025−6033. (c) Jursic, B. S. *THEOCHEM* **1998**, *423*, 189−194. (d) Jensen, F.; Houk, K. N. *J. Am. Chem. Soc.* **1987**, *109*, 3139−3140.

(18) For comparative purposes, we have also optimized the transition state corresponding to the [1,5]-H migration in 1,3-pentadiene, although it has been extensively studied previously by others (see ref 17 and references cited herein).

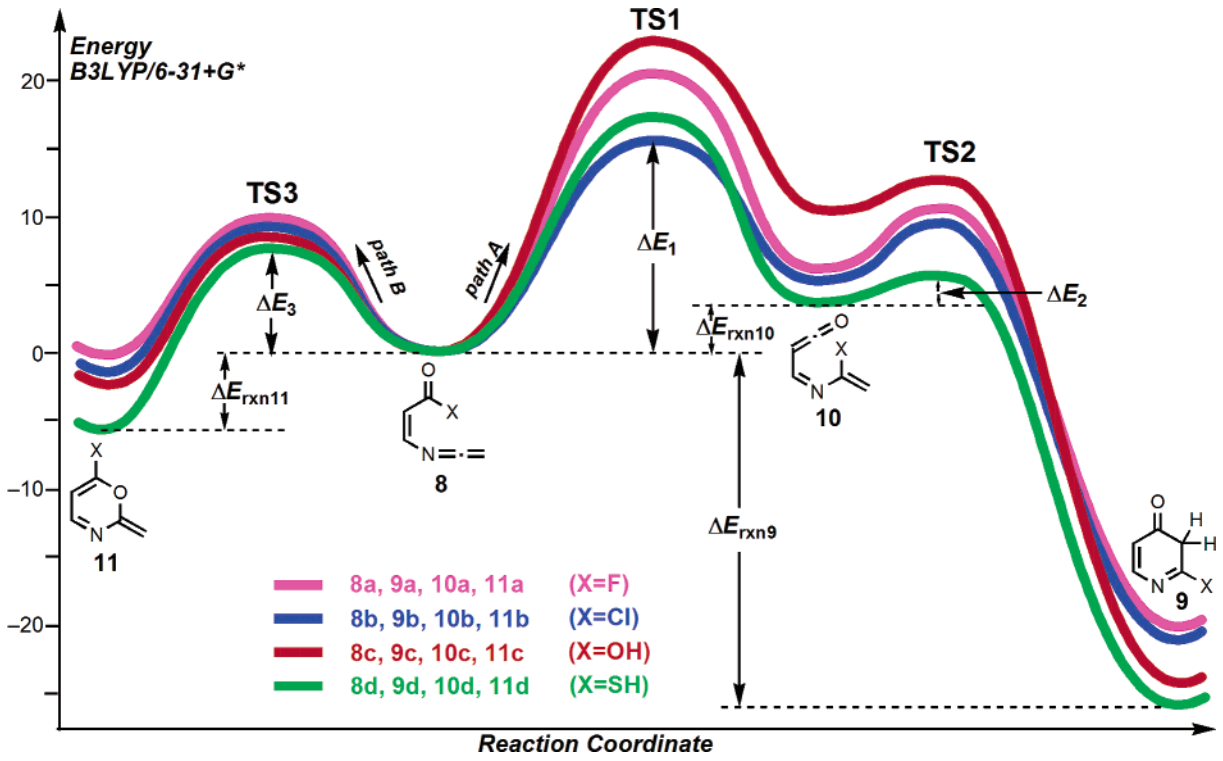


**FIGURE 1.** Qualitative reaction profiles at the B3LYP/6-31+G* level for the transformation of the ketenimines **8a**−**d** into the 4(3*H*)-pyridones **9a**−**d** and the 1,3-oxazines **11a**−**d**.

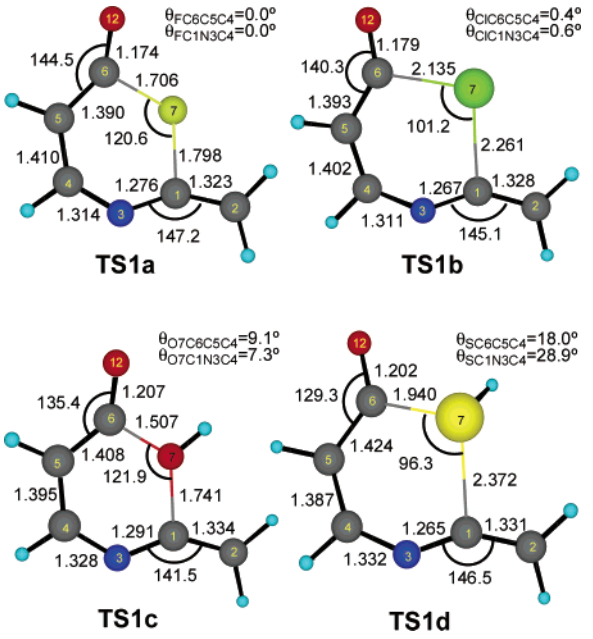


**FIGURE 2.** B3LYP/6-31+G*-optimized geometries of the transition structures found in the transformation of the ketenimines **8a**−**d** into the ketenes **10a**−**d**.

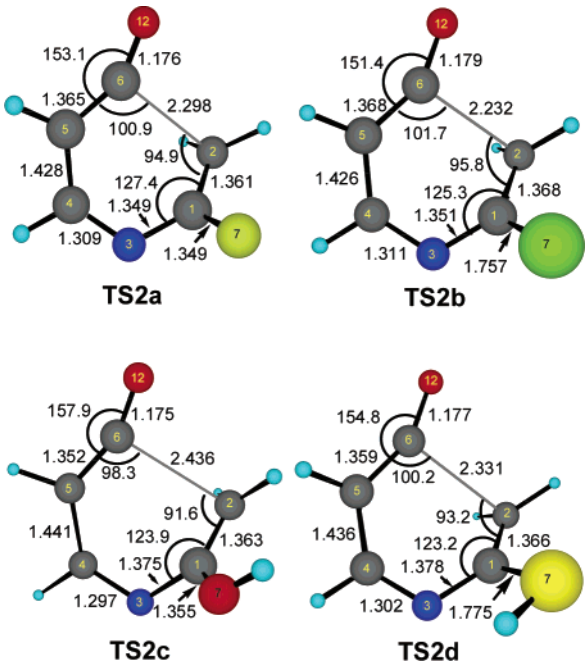


**FIGURE 3.** B3LYP/6-31+G*-optimized geometries of the transition structures found in the cyclization of the ketenes **10a**−**d** to the 4(3*H*)-pyridones **9a**−**d**.

the 4(3*H*)-pyridones **9a**−**d** are unusually small. The geometries of **TS2a**−**d** show their monorotatory nature (the hydrogen at C5, C4, C5, C6, and O12 are in the same plane; see Figure 3). The analysis of the imaginary frequency associated with each transition structure revealed that the nuclear movements do not involve rotation around the C5−C6 $\pi$ system but only around the C1−C2 ones. Both, the geometry of the transition states **TS2a**−**d** and the small values of the energy barriers indicate that their orbital topology could be qualified as pseudopericyclic (see below).

**Two-Step [1,5]-X Sigmatropic Rearrangement of Ketenimines 8e,f to Ketenes 10e,f and Subsequent 6$\pi$-Electrocyclic Ring Closure Leading to 4(3*H*)-Pyridones 9e,f.** The intensive search along the HF/6-31G* potential energy surface associated

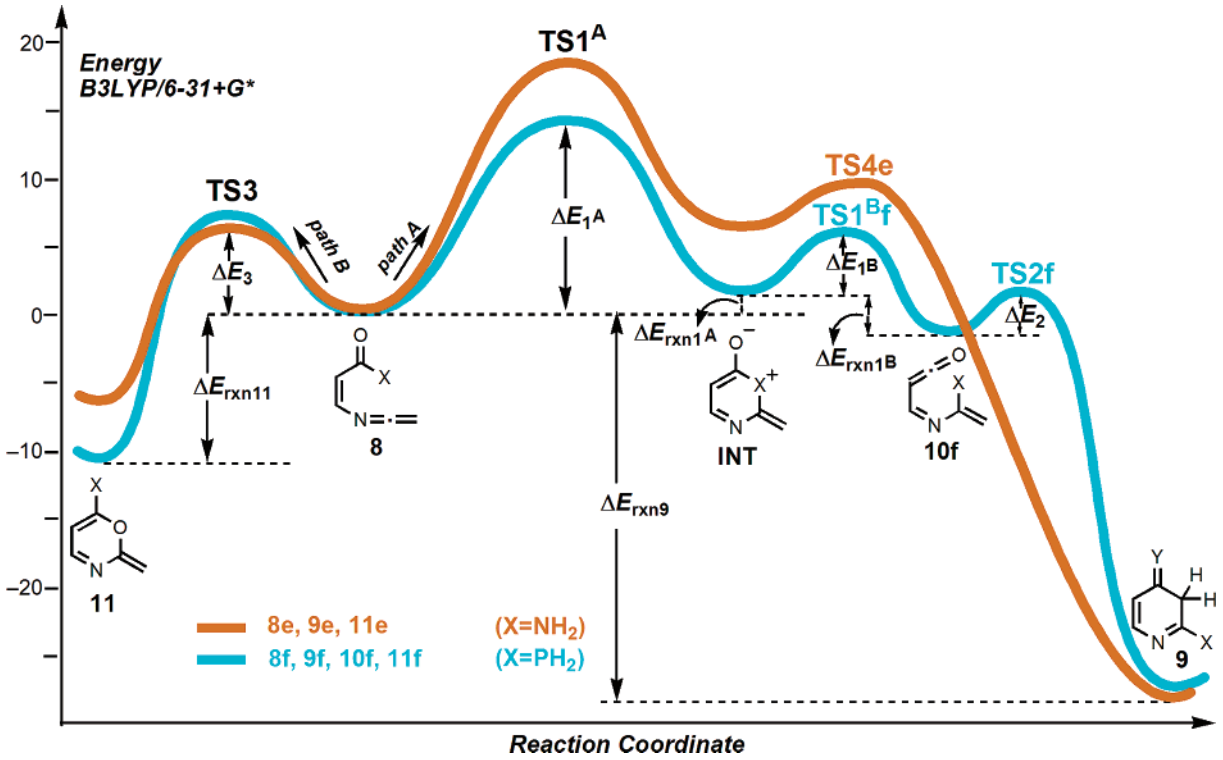


**FIGURE 4.** Qualitative reaction profiles at the B3LYP/6-31+G* level for the transformation of the ketenimines **8e**,**f** into the 4(3*H*)-pyridones **9e**,**f** and the 1,3-oxazines **11e**,**f**.

with the transformation of ketenimines **8e** and **8f** into the 4(3*H*)-pyridones **9e** and **9f** revealed that the [1,5]-migration of the $NH_2$ and $PH_2$ groups leading to the ketene intermediates does not occur in a concerted mode, but instead taking place in two steps.[20] The first one consists of the nucleophilic attack of the lone pair at the nitrogen or phosphorus atom onto the central carbon atom of the ketenimine moiety, through the transition structures **TS1$^{A}$e**,**f**, to provide the dipolar intermediates **INTe**,**f**. In a second step the breaking of the C6−X bond takes place, via the transition states **TS1$^{B}$e**,**f**, leading to the ketenes **10e**,**f** (see Scheme 5). The ability of nitrogen and phosphorus to exist in a tetracoordinated state could explain why in these cases the [1,5]-shift takes place involving the formation of the zwitterionic intermediates. The ring closure of ketenes **10e**,**f** occurs via the transition states **TS2e**,**f**, whose geometries are analogous to those found in **TS2a**−**d**. The exploration of the potential energy surface at the correlated B3LYP/6-31+G* level led to the same results, except for **TS1$^{B}$e**, the ketene intermediate **10e**, and the transition structure **TS2e**, which could not be optimized at that theoretical level. Instead, we found only a transition structure **TS4e** involving the simultaneous breaking of the C6−N7 bond and the formation of the C2−C6 bond. The IRC calculations showed that **TS4e** connects with the dipolar intermediate **INTe** and the 2-amino-4(3*H*)-pyridone **9e** (see Scheme 6 and path A in Figure 4).

At the B3LYP/6-31+G* theoretical level the computed energy barriers for the formation of the polar intermediates **INTe**,**f** from the ketenimines **8e**,**f** were 18.09 and 14.38 kcal·mol$^{-1}$ respectively, both processes being slightly endothermic. The energy barrier for the breaking of the C6−P7 bond in **INTf**, leading to the ketene **10f**, is very low (3.52 kcal·mol$^{-1}$). The conversion **INTe**→**10e**, at the HF/6-31G* theoretical level, involves an almost imperceptible barrier (0.64 kcal·mol$^{-1}$). At the B3LYP/6-31+G* level, the energy barrier calculated for the transformation of the polar intermediate **INTe** into 2-amino-4(3*H*)-pyridone (**9e**), via the transition structure **TS4e**, was only 3.45 kcal·mol$^{-1}$. The overall processes transforming the ketenimines **8e**,**f** into the final 4(3*H*)-pyridones **9e**,**f** are exothermic by 27.58 and 27.44 kcal·mol$^{-1}$, respectively. The stationary points of these transformations are represented in Figures 5 and 6.

At this point, we can establish, according to the energy barriers computed for the [1,5]-shifts studied in this work (see $\Delta E_1$ and $\Delta E_1^{A}$ in Table 2), the order of migratory aptitudes of the X substituents at the acyl group in ketenimines **8a**−**f**, which is predicted to be, from highest to lowest, the following: $PH_2$ > Cl > SH > $NH_2$ > F> OH.

The groups based on the second-row elements ($PH_2$, Cl, SH) show higher migratory aptitude than those based on first-row elements ($NH_2$, F, OH), a fact that can be rationalized by taking into account the values of the C−X bond dissociation energies, which are smaller for C−P, C−Cl, and C−S than for C−N, C−F, and C−O, respectively. On the other hand, as these [1,5]-

(19) (a) Rodríguez-Otero, J. *J. Org. Chem.* **1999**, *64*, 6842−6848. (b) Jiao, H.; Schleyer, P. v. R. *J. Am. Chem. Soc.* **1995**, *117*, 11529−11535. (c) Evanseck, J. D.; Thomas, B. E., IV; Spellmeyer, D. C.; Houk, K. N. *J. Org. Chem.* **1995**, *60*, 7134−7141. (d) Jefford, C. W.; Bernardinelli, G.; Wang, Y.; Spellmeyer, D. C.; Buda, A.; Houk, K. N. *J. Am. Chem. Soc.* **1992**, *114*, 1157−1165. (e) Baldwin, J. E.; Reddy, V. P.; Schaad, L. J.; Hess, B. A. *J. Am. Chem. Soc.* **1988**, *110*, 8554−8555.

(20) (a) An analogous finding was accomplished in the study of the effect of several substituents in the vinylketene−acylallene rearrangement reported by Wentrup et al.: the [1,3]-shift in the dimethylamino group takes place involving the formation of a zwitterionic intermediate. See: Bibas, H.; Wong, M. W.; Wentrup, C. *Chem.-Eur. J.* **1997**, *3*, 237−248. (b) Recently, Wentrup et al. have also found zwitterionic intermediates in the [1,3]-shifts of amino and dimethylamino groups in the imidoylketene−acyl ketenimine rearrangement; see: Finnerty, J. F.; Wentrup, C. *J. Org. Chem.* **2005**, *70*, 9735−9739.

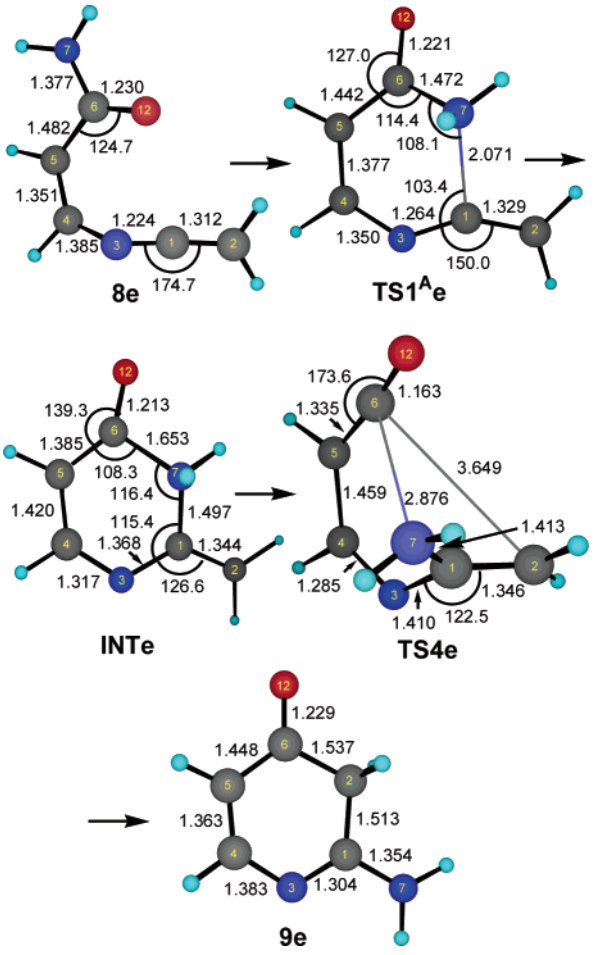


**FIGURE 5.** B3LYP/6-31+G*-optimized geometries of the stationary points found in the cyclization of the ketenimine **8e** to the 4(3*H*)-pyridone **9e**.

shifts involve the interaction between a high-lying orbital of the migrating group and the low-lying LUMO of the ketenimine (see below), the activation barriers depending on the respective nucleophilicities and electrophilicities of the reacting centers. Therefore, as the second-row elements are known to be more nucleophilic than those of the first-row, this fact serves to explain why the energy barriers for the migration of the second-row atoms are lower than those of their first-row isovalent counterparts.

It is worthy to remark here that Wentrup and others have systematically studied a number of equilibria between acyl ketenimines and imidoyl ketenes by sigmatropic [1,3]-rearrangements of H and other atoms or groups and established their pseudopericyclic nature and the relative migratory aptitude of different groups.[20a,21] However, [1,5]-sigmatropic rearrangements in heterocumulenes as such here reported have not been disclose up to now.

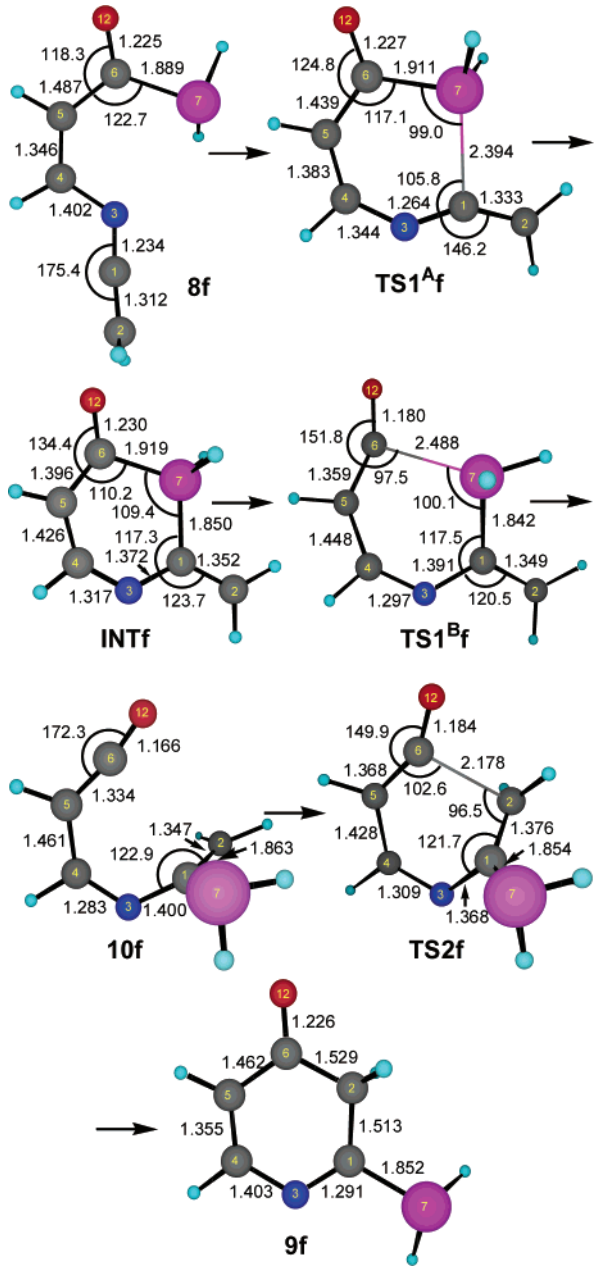


**FIGURE 6.** B3LYP/6-31+G*-optimized geometries of the stationary points found in the cyclization of the ketenimine **8f** to the 4(3*H*)-pyridone **9f**.

**Path B: Cyclization of Ketenimines 8a−f to the 1,3-Oxazines 11a−f.** Our calculations show that the alternative mode of cyclization of the ketenimines **8a−f**, its 6$\pi$-electrocyclic ring closure leading to 2-methylene-6-substituted-1,3-oxazines **11a−f**, takes place via the transition structures **TS3a−f** (Figure 7). Interestingly, the geometry of all these transition structures is planar, and the analysis of their imaginary frequencies showed the nonrotatory nature of these cyclizations. The computed energy barriers ($\Delta E_3$) are very low (from 6.35 to 9.62 kcal·mol$^{-1}$), and their exothermicities range from 0.22 to 11.85 kcal·mol$^{-1}$.

From the reaction profiles in Figures 1 and 4 and the values of the energy barriers gathered in Table 2, the following conclusions can be drawn: (i) the 4(3*H*)-pyridones **9a−f** are predicted to be the thermodynamically controlled products,

(21) (a) Koch, R.; Wentrup, C. *Org. Biol. Chem.* **2004**, *2*, 195−199. (b) Nguyen, M. T.; Landuyt, L.; Nguyen, H. M. T. *Eur. J. Org. Chem.* **1999**, 401−407. For similar [1,3]-sigmatropic shifts occurring in other heterocumulenes see: (c) Koch, R.; Wentrup, C. *J. Chem. Soc., Perkin Trans. 2* **2000**, 1846−1850. (d) Ammann, J. R.; Flammang, R.; Wong, M. W.; Wentrup, C. *J. Org. Chem.* **2000**, *65*, 2706. (e) Wong, M. W.; Wentrup, C. *J. Org. Chem.* **1994**, *59*, 5279−5285. (f) Bibas, H.; Wong, M. W.; Wentrup, C. *J. Am. Chem. Soc.* **1995**, *117*, 9582−9583. (g) Finnerty, J.; Andraos, J.; Yamamoto, Y.; Wong, M. W.; Wentrup, C. *J. Am. Chem. Soc.* **1998**, *120*, 1701−1704.

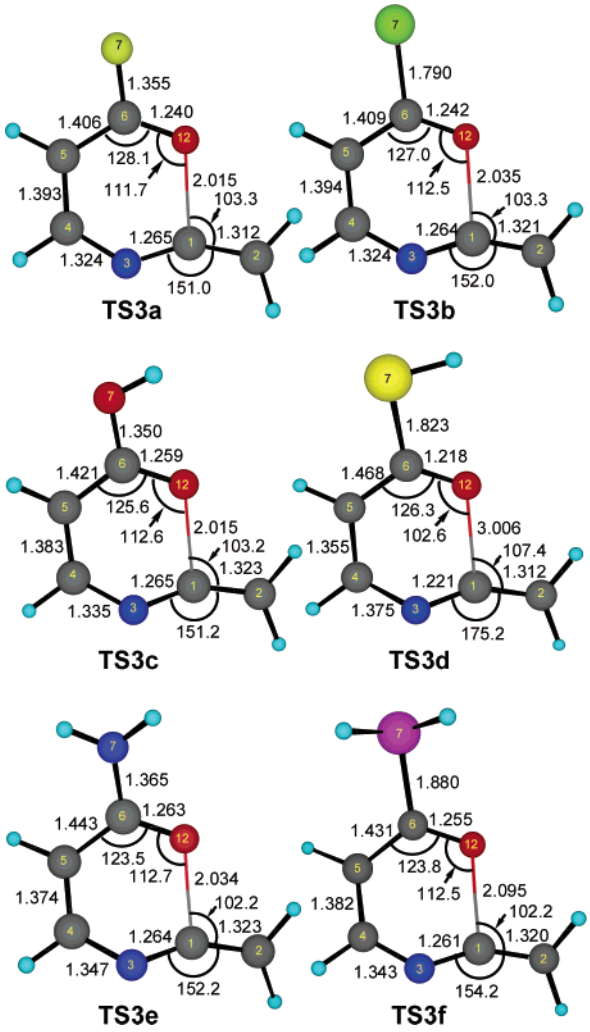


**FIGURE 7.** B3LYP/6-31+G*-optimized geometries of the transition structures found in the cyclization of the ketenimines **8a**−**f** to the 1,3-oxazines **11a**−**f**.

whereas the 1,3-oxazines **11a**−**f** should be the kinetically controlled ones; (ii) in the cyclization of ketenimines **8a**−**d** leading to the 4(3*H*)-pyridones **9a**−**d**, the first step (the [1,5]-X shift, X = F, Cl, OH or SH) is rate-limiting; (iii) in the cyclization of ketenimines **8e**,**f** leading to the 4(3*H*)-pyridones **9e**,**f** (X = $NH_2$, $PH_2$), the first step leading to the corresponding zwitterionic intermediates (**INTe**,**f**) is rate-limiting (note that when X = $NH_2$, $PH_2$, the 1,5-shift takes place in a two-step process through the formation of such intermediates). Therefore, the exclusive formation of quinolin-4(3*H*)-ones **5** in the experiments described above (modeled by the 4(3*H*)-pyridones **9** in the theoretical study) can be rationalized as resulting from the prevalence of the mechanistic pathway A of Scheme 3 under thermodynamic control.

A qualitative measuring of the reaction time required for the total transformation of the 1,3-oxazines **11** into the pyridones **9** can be inferred from the energy barriers gathered in Table 2. From the addition of $\Delta E_1$ and ($-\Delta E_{rxn11}$) the order of reaction times required for the different groups X is predicted to be, from lowest to highest, the following: Cl < F < SH < $NH_2$ ≤ OH < $PH_2$.

In the ketenimines **8a**−**f** used in the computational study, the vinyl group joining the acyl and ketenimine functions models the benzene ring of the ketenimines **4**. The lack of this benzene ring does not account for the loss of aromaticity, which is expected to take place in both the sigmatropic rearrangement of ketenimines **4** leading to ketenes **6** and the 6$\pi$-electrocyclization to lead to the benzoxazines **7**. Therefore, it is expected that the corresponding energy barriers for the transfomation of ketenimines **4** into the quinolin-4(3*H*)-ones **5** and the benzoxazine **7** will be higher than those obtained in the computational study. However, we believe that this fact does not affect significantly the results of the computational study, as the penalty for sacrificing the aromaticity would be similar for both processes.[22] But, more notably, the benzoxazines **7** might be more unstable, on thermodynamic grounds, than the corresponding oxazines **11**, and accordingly, the barrier for the conversion of benzoxazines **7** into the corresponding quinolin-4(3*H*)-ones **5** would essentially be the barrier between **4** and **6**, i.e., that corresponding to the [1,5]-X shift (note that, due to the retrieval of aromaticity, the barrier for the conversion of ketenes **6** into the quinolin-4(3*H*)-ones **5** it is expected to be lower than that of ketenes **10** into the 4(3*H*)-pyridones **9**).

**Characterization of the Pseudopericyclic Topology of the Transition States TS1, TS2, and TS3.** An added value to the study of the mechanistic scheme for the two cyclization modes of the ketenimines **8** is the characterization of the transition states involved in these transformations as pseudopericyclic or not. Before elucidating the mechanistic pathways, we already pointed out that the structure of the ketenimines **8** enables these processes to show pseudopericyclic characteristics.[23]

The characterization of a process as pseudopericyclic has been usually established on the basis of the planar or nearly planar geometry of the corresponding transition state.[23b−f,24] In several reports, the second-order perturbation interactions[25] and the bond order values of the NLMOs,[25f,j] from the NBO (natural bond orbital) analyses, have been used to show the disconnections in the orbital overlap of the transition states. The ACID method, by Herges et al.,[26] has also proved to be a useful tool in the discrimination between pericyclic and pseudopericyclic pathways,[25d,f,27] and recently, the topological analysis of the electron localization function (ELF) has been proposed with this aim.[28]

(22) The penalty for sacrificing the aromaticity in related [1,5]-shifts in ketenimines is around 10 kcal·mol$^{-1}$; see ref 12.

(23) Pseudopericyclic reactions lack cyclic orbital overlap and have four characteristics, as stated by Birney: (1) all are allowed, (2) they have nonaromatic transition states, (3) they may have very low barriers, and (4) they may have planar transition states. (a) For Lemal's definition of a pseudopericyclic process, see: Ross, J. A.; Seiders, R. P.; Lemal, D. M. *J. Am. Chem. Soc.* **1976**, *98*, 4325−4327. For other examples of pseudopericyclic reactions, see, for example: (b) Birney, D. M.; Wagenseller, P. E. *J. Am. Chem. Soc.* **1994**, *116*, 6262−6270. (c) Birney, D. M. *J. Org. Chem.* **1994**, *59*, 2557−2564. (d) Wagenseller, P. E.; Birney, D. M.; Roy, *J. Org. Chem.* **1995**, *60*, 2853−2859. (e) Birney, D. M. *J. Org. Chem.* **1996**, *61*, 243−251. (f) Birney, D. M.; Xu, X.; Ham, S. *Angew. Chem., Int. Ed.* **1999**, *38*, 189−193. (g) Alajarín, M.; Sánchez-Andrada, P.; Cossío, F. P.; Arrieta, A.; Lecea, B. *J. Org. Chem.* **2001**, *66*, 8470−8477.

(24) See, for example: (a) Bornemann, H.; Wentrup, C. *J. Org. Chem.* **2005**, *70*, 5862−5868. (b) Wei, H.-X.; Zhou, C.; Ham, H.; White, J. M.; Birney, D. M. *Org. Lett.* **2004**, *6*, 4289−4292. (c) Birney, D. M. *Org. Lett.* **2004**, *6*, 851−854. (d) Birney, D. M. *J. Am. Chem. Soc.* **2000**, *122*, 10917−10925. (e) Shumway, W.; Ham, S.; Moer, J.; Wittlesey, B. R.; Birney, D. M. *J. Org. Chem.* **2000**, *65*, 7731−7739. (f) Alajarín, M.; Vidal, A.; Sánchez-Andrada, P.; Tovar, F.; Ochoa, G. *Org. Lett.* **2000**, *2*, 965−968. (g) Bibas, H. K.; Wentrup, C. *J. Org. Chem.* **1998**, *63*, 2619−2626. (h) Birney, D. M.; Ham, S.; Unruh, G. R. *J. Am. Chem. Soc.* **1997**, *119*, 4509−4517. (i) Luo, L.; Bartberger, M. D.; Dolbier, W. R., Jr. *J. Am. Chem. Soc.* **1997**, *119*, 12366−12367. (j) Ham, S.; Birney, D. M. *J. Org. Chem.* **1996**, *61*, 3962−3968. (k) Koch, R.; Wong, M. H.; Wentrup, C. *J. Org. Chem.* **1996**, *61*, 6809−6813. (l) Wagenseller, P. E.; Birney, D. M.; Roy, D. *J. Org. Chem.* **1995**, *60*, 2853−2859.

**TABLE 2. Energy Barriers[a] ($\Delta E$, kcal·mol$^{-1}$) Computed for the Alternative Cyclization Modes of Ketenimines 8a−f Leading to 9a−f and 11a−f[b]**

| method | $\Delta E_1$ | $\Delta E_2$ | $\Delta E_3$ | $\Delta E_{rxn10}$ | $\Delta E_{rxn9}$ | $\Delta E_{rxn11}$ |
|---|---|---|---|---|---|---|
| | | | **8a→9a/11a** (X = F) | | | |
| HF/6-31G*[c] | 37.30 | 15.14 | 18.84 | 7.40 | −24.17 | −1.48 |
| B3LYP/6-31+G*[d] | 21.47 | 5.20 | 9.62 | 6.33 | −20.09 | −0.22 |
| | | | **8b→9b/11b** (X = Cl) | | | |
| HF/6-31G*[c] | 31.25 | 16.38 | 17.98 | 2.11 | −28.23 | −5.62 |
| B3LYP/6-31+G*[d] | 15.76 | 3.50 | 9.06 | 5.54 | −21.62 | −2.49 |
| | | | **8c→9c/11c** (X = OH) | | | |
| HF/6-31G*[c] | 35.04 | 11.68 | 17.75 | 12.07 | −27.44 | −2.77 |
| B3LYP/6-31+G*[d] | 22.90 | 2.76 | 8.50 | 10.23 | −24.14 | −2.65 |
| | | | **8d→9d/11d** (X = SH) | | | |
| HF/6-31G*[c] | 35.17 | 13.52 | 16.43 | 0.70 | −31.01 | −8.63 |
| B3LYP/6-31+G*[d] | 16.75 | 1.51 | 7.62 | 3.56 | −25.36 | −6.03 |

| method | $\Delta E_1^A$ | $\Delta E_1^B$ | $\Delta E_2$ | $\Delta E_3$ | $\Delta E_{rxn1}^A$ | $\Delta E_{rxn1}^B$ | $\Delta E_{rxn9}$ | $\Delta E_{rxn11}$ |
|---|---|---|---|---|---|---|---|---|
| | | | | **8e→9e/11e** (X = $NH_2$) | | | | |
| HF/6-31G*[c] | 29.63 | 0.64 | 6.02 | 14.59 | 14.75 | −6.47 | −30.41 | −7.80 |
| B3LYP/6-31+G*[d] | 18.09 | 3.45 | | 6.35 | 5.77 | − | −27.58 | −7.09 |
| | | | | **8f→9f/11f** (X = $PH_2$) | | | | |
| HF/6-31G*[c] | 32.46 | 2.78 | 17.00 | 16.42 | 14.16 | −18.59 | −32.70 | −14.11 |
| B3LYP/6-31+G*[d] | 14.38 | 3.52 | 4.12 | 6.47 | 1.80 | −4.23 | −27.44 | −11.85 |

[a] The energy barriers $\Delta E_1$, $\Delta E_3$, and $\Delta E_1^A$ have been calculated from the most stable conformer (around the C3−C4 and the C5−C6 single bonds) of ketenimines **8a−f**, as usual. [b] See Figures 1 and 4 for the notation of the energy barriers. [c] Energies computed on the fully optimized HF/6-31G* geometries. The ZPVE corrections, computed at the same level, have been included. The ZPEs were not scaled. [d] Energies computed on the fully optimized B3LYP/6-31+G* geometries. The ZPVE corrections, computed at the same level, have been included. The ZPEs were not scaled.

**SCHEME 5. Mechanistic Scheme Found at the HF/6-31G* Theoretical Level for the Cyclization of the Ketenimines 8e,f to the 4(3*H*)-Pyridones 9e,f[a]**

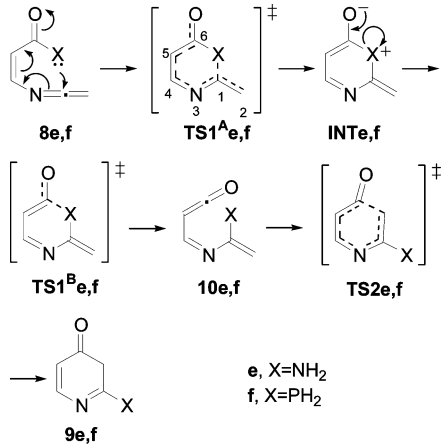


[a] For **8f** (X = $PH_2$), the same mechanistic pathway was found at the B3LYP/6-31+G* level.

One of the recognized characteristics of the pseudopericyclic reactions is that they occur through nonaromatic transition states as the orbital disconnections prevent the aromaticity. Accordingly, the study of the magnetic properties of the transitions states and their relation with aromaticity is one of the most useful criteria to distinguish between pericyclic and pseudopericyclic mechanisms, particularly the analysis of its nuclear independent chemical shift (NICS) values pioneered by Schleyer et al.,[29] who showed that large negative NICS values at the center of the ring under consideration are associated with aromatic character, whereas positive NICS values are a convenient indicator of antiaromaticity. Cossío et al.,[30] and afterward some of us,[16,23g,25b] have found that the magnetic behavior of aromatic compounds or transition states can be described by the variation of the NICS at different points above and below the molecular plane, the intersection point being the (3,+1) ring critical point as defined by Bader.[31] Currently, the NICS values at different points are frequently used to distinguish between pericyclic and pseudopericyclic transition states.[13,25d,f,27b,c,32] The ring current model and the magnetic criteria, as showed by Cossío et al., also allow the distinction among different kinds of aromaticity: $\sigma$-, $\pi^1$-, and $\pi^2$-aromaticity.[30e]

**SCHEME 6. Mechanistic Scheme Found at the B3LYP/6-31+G* Theoretical Level for the Cyclization of the Ketenimine 8e to the 4(3*H*)-Pyridones 9e**

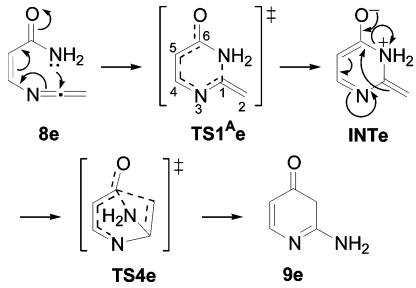


On the basis of the geometries of **TS1a−d**, **TS2a−f**, and **TS3a−f** and the results of the second-order perturbation

(25) (a) Sadavisam, D. V.; Birney, D. M. *Org. Lett.* **2005**, *7*, 5817−5820. (b) Alajarín, M.; Sánchez-Andrada, P.; López-Leonardo, C.; Álvarez, A. *J. Org. Chem.* **2005**, *70*, 7617−7623. (c) Fukushima, K.; Iwahashi, H. *Heterocycles* **2005**, *65*, 2605−2618. (d) Cabaleiro-Lago, E. M.; Rodríguez-Otero, J.; González-López, I.; Peña-Gallego, A.; Hermida-Ramón, J. M. *J. Phys. Chem. A* **2005**, *109*, 5636−5644. (e) Zhou, C.; Birney, D. M. *J. Org. Chem.* **2004**, *69*, 86−89. (f) Peña-Gallego, A.; Rodríguez-Otero, J.; Cabaleiro-Lago, E. M. *J. Org. Chem.* **2004**, *69*, 7013−7017. (g) Rodriguez-Otero, J.; Cabaleiro-Lago, E. M. *Chem.-Eur. J.* **2003**, *9*, 1837−1843. (h) De Lera, A. R.; Cossío, F. P. *Angew. Chem., Int. Ed.* **2002**, *41*, 1150−1152. (i) Zhou, C.; Birney, D. M. *J. Am. Chem. Soc.* **2002**, *124*, 5231−5241. (j) Fabian, W. M. F.; Kappe, C. O.; Bakulev, V. A. *J. Org. Chem.* **2000**, *65*, 47−53. (k) Fabian, W. M. F.; Bakulev, V. A.; Kappe, C. O. *J. Org. Chem.* **1998**, *63*, 5801−5805.

(26) (a) Herges, R.; Geuenich, D. *J. Phys. Chem. A* **2001**, *105*, 3214−3220. (b) Herges, R.; Papafilippopoulos, A. *Angew. Chem., Int. Ed.* **2001**, *40*, 4671−4674. (c) Kimball, D. B.; Herges, R.; Haley, M. M. *J. Am. Chem. Soc.* **2002**, *124*, 1572−1573.

analyses, showing the delocalization energies of electrons from filled into empty NBOs, and the study of their magnetic properties, we have been able to establish the pseudopericyclic nature of these transition states. The optimized geometries of **TS1a**−**d**, **TS2a**−**f**, and **TS3a**−**f** at the B3LYP/6-31+G* level showing the points used to evaluate the NICS values are depicted in the Figures S1−S3 of the Supporting Information.

**Transition Structures TS1a**−**d.** The NBO analysis of these transition structures shows the new, partially formed $\sigma$C1−X7 bond resulting mainly from the interaction between a lone pair of the migrating heteroatom (which changes from a nonbonding $sp^2$ orbital to a bonding $sp^3$ orbital) and a p orbital of the C1═N3 system (the LUMO of the ketenimine moiety placed in the molecular plane) and not from the interaction between the $\sigma$C6−X bond and the $\pi$C1═N3 system expected for a transition state of pericyclic nature (see selected interactions from the second-order perturbation analyses in the Supporting Information). The initial $sp^2$ $\sigma$C6−X bond orbital changes to a nonbonding $sp^3$ orbital for accommodating a lone pair in the migrating heteroatom of the final product. From these orbital disconnections the pseudopericyclic topology of these transition structures (**TS1a**−**d**) can thus be envisaged. These [1,5]-shifts can be viewed as a swing of a negative group (the migrating heteroarom) between the two positive termini (C1 and C6).

We will now deal with the magnetic properties of the transition states **TS1a**−**d**. To our knowledge, there are no precedents on the characterization as pseudopericyclic of [1,5]-shifts on the basis of the magnetic behavior of the corresponding transition states. With the aim of comparing the magnetic properties of **TS1a**−**d** with an adequate model of pericyclic [1,5]-shift, we have selected the transition state **TS1ref** corresponding to the [1,5]-H shift in (*Z*)-1,3-pentadiene. Schleyer and Jiao, in their seminal publication in which they showed magnetic evidence of the aromaticity of pericyclic transition structures,[33] demonstrated that the NICS value (−16.6 ppm) at the geometrical center of that transition state agrees with their high aromaticity, previously established on the basis of geometric, energetic, and others magnetic criteria.[34] We have also optimized **TS1ref** and calculated the NICS values along the *z*-axis perpendicular to the molecular plane which intersects the (3,+1) critical point. According to the behavior of the diamagnetic shielding along this *z*-axis in **TS1ref** (see Figure 8A), we propose to classify the aromaticity of **TS1ref** as $\pi^1$-aromaticity, as there is only one maximum diamagnetic shielding above the molecular plane, which corresponds to the ring current circulating on the side where the suprafacial transfer of hydrogen allows a close proximity between the p atomic orbitals. The plot of the NICS values versus *z* for the transition structures **TS1a**−**d** differs notably from that found for **TS1ref**, and the computed NICS values at the RCP ($NICS_{RCP}$) and the maximum NICS values ($NICS_{max}$) of **TS1a**−**d** are much lower than those expected for an aromatic transition state. These results can be seen in Table 3 and Figure 8A. Consequently, the transition structures **TS1a**−**d** are clearly nonaromatic, confirming their pseudopericyclic nature.

At this point, it is worth recalling the scarce precedents of pseudopericyclic [1,5]-shifts that have been reported so far.[23e,24g,24k,25b,e,i,35] Among these processes, there are only a few examples taking place in heterocumulenes: the degenerated chlorine[24k] and hydrogen[23e,35] rearrangement of $\beta$-(chlorocarbonyl)vinyl ketene and $\beta$-(formyl)vinyl ketene, respectively, and the [1,5]-H shift in 1-propenyl ketene.[24g] The pseudopericyclic character of these transition states has been established on the basis of their planar geometries.

**Transition Structures TS2a**−**f.** The forming $\sigma$-bond C2−C6 in **TS2a**−**f** is mainly due to the interaction between the $\pi$C1−C2 and the $\pi$*C6−O12 (the LUMO of the ketene fragment placed in the molecular plane) natural localized orbitals (see Supporting Information), instead of the interaction between the natural localized orbitals $\pi$C1−C2/$\pi$*C5−C6 and $\pi$C5−C6/$\pi$*C1−C2 expected for a transition state of pericyclic topology. Besides, the p orbital at the ketene oxygen atom rehybridizes to an $sp^2$ orbital to accommodate a lone pair in the final product, whereas the new $\pi$C═O system results from the interaction between a lone pair at the oxygen atom and the p orbital at C6 perpendicular to the molecular plane. Therefore, there are disconnections in the C═O terminus. Obviously, in the C5═C6 end no role interchange between nonbonding and bonding orbitals can take place, explaining the monorotatory nature of these transition structures as showed by their geometries. Again, the pseudopericyclic topology of these transition states (**TS2a**−**f**) was confirmed by their magnetic properties (see Table 3 and Figure 8B). We selected as the aromatic model for a pericyclic 6$\pi$-electrocyclization the transition state corresponding to the cyclization of *cis*-1,3,5-hexatriene to 1,3-cyclohexadiene, **TS2ref**. The shape of the plot curve (NICS versus *z*) for **TS2ref**, whose aromaticity was defined by Cossío et al. as the prototype of $\pi^1$-aromaticity,[30e] differs substantially of those obtained for **TS2a**−**f** (Figure 8B). Also, the low $NICS_{RCP}$ and $NICS_{max}$ values clearly indicate the nonaromaticity of these transition states and point to its pseudopericyclic nature.

(27) (a) Kimball, D. M.; Weakley, T. J. R.; Herges, R.; Haley, M. M. *J. Am. Chem. Soc.* **2002**, *124*, 13463−13473. (b) Cabaleiro-Lago E. M.; Rodríguez-Otero, J.; García-López, R. M.; Peña-Gallego, A.; Hermida-Ramón, J. M. *Chem.- Eur. J.* **2005**, *11*, 5966−5974. (c) Cabaleiro-Lago, E. M.; Rodríguez-Otero, J.; Varela-Varela, S. M.; Peña-Gallego, A.; Hermida-Ramón, J. M. *J. Org. Chem.* **2005**, *70*, 3921−3928. (d) Peña-Gallego, A.; Rodríguez-Otero, J.; Cabaleiro-Lago, E. M. *Eur. J. Org. Chem.* **2005**, 3228−3232.

(28) (a) Chamorro, E. E.; Notario, R. *J. Phys. Chem. A* **2004**, *108*, 4099−4104. (b) Cárdenas, C.; Chamorro, E.; Notario, R. *J. Phys. Chem. A* **2005**, *109*, 4352−4358. (c) Matito, E.; Sola, M.; Duran, M.; Poater, J. *J. Phys. Chem. B* **2005**, *109*, 7591−7593. (d) Rode, J. E.; Dobrowolski, J. Cz. *J. Phys. Chem. A* **2006**, *110*, 207−218.

(29) (a) Schleyer, P. v. R.; Maerker, C.; Dransfeld, A.; Jiao, H.; Hommes, N. J. R. v. E. *J. Am. Chem. Soc.* **1996**, *118*, 6317−6318. (b) Schleyer, P. v. R.; Jiao, H.; Hommes, N. J. R. v. E.; Malkin, V. G.; Malkina, O. L. *J. Am. Chem. Soc.* **1997**, *119*, 12669−12670. (c) Schleyer, P. v. R.; Manoharn, M.; Wang, Z.-X.; Kiran, B.; Jiao, H.; Puchta, R.; Hommes, N. J. R. v. E. *Org. Lett.* **2001**, *3*, 2465−2468. (d) See also Fallah-Bagher-Shaidaei, H.; Wannere, C. S.; Corminboeuf, C.; Puchta, R.; Schleyer, P. v. R. *Org. Lett.* **2005**, *7*, 863−866 and references herein.

(30) (a) Morao, I.; Lecea, B.; Cossío, F. P. *J. Org. Chem.* **1997**, *62*, 7033−7036. (b) Morao, I.; Cossío, F. P. *J. Org. Chem.* **1999**, *64*, 1868−1874. (c) Cossío, F. P.; Morao, I.; Jiao, H.; Scheleyer, P. v. R. *J. Am. Chem. Soc.* **1999**, *121*, 6737−6746. (d) Vivanco, S.; Lecea, B.; Arrieta, A.; Prieto, P.; Morao, I.; Linden, A.; Cossío, F. P. *J. Am. Chem. Soc.* **2000**, *122*, 6078−6092. (e) de Lera, A. R.; Alvarez, R.; Lecea, B.; Torrado, A.; Cossío, F. P. *Angew. Chem., Int. Ed.* **2001**, *40*, 557−561.

(31) Bader, R. F. W. *Atoms in Molecules*—A Quantum Theory; Clarendon Press: Oxford, 1990; pp 13−52.

(32) See, for example: (a) Montero-Campillo, M. M.; Rodríguez-Otero, J.; Cabaleiro-Lago, E. M. *J. Phys. Chem. A* **2004**, *108*, 8373−8377. (b) Zora, M. *J. Org. Chem.* **2004**, *69*, 1940−1947. (c) Cossío, F. P.; Alonso, C.; Lecea, B.; Ayerbe, M.; Rubiales, G.; Palacios, F. *J. Org. Chem.* **2006**, *71*, 2839−2847.

(33) Jiao, H.; Schleyer, P. v. R. *J. Chem. Soc., Faraday Trans.* **1994**, *90*, 1559−1567.

(34) Jiao, H.; Schleyer, P. v. R. *J. Phys. Chem.* **1998**, *11*, 655−662.

(35) Reva, I.; Breda, S.; Roseiro, T.; Eusebio, E.; Fausto, R. *J. Org. Chem.* **2005**, *70*, 7701−7710.

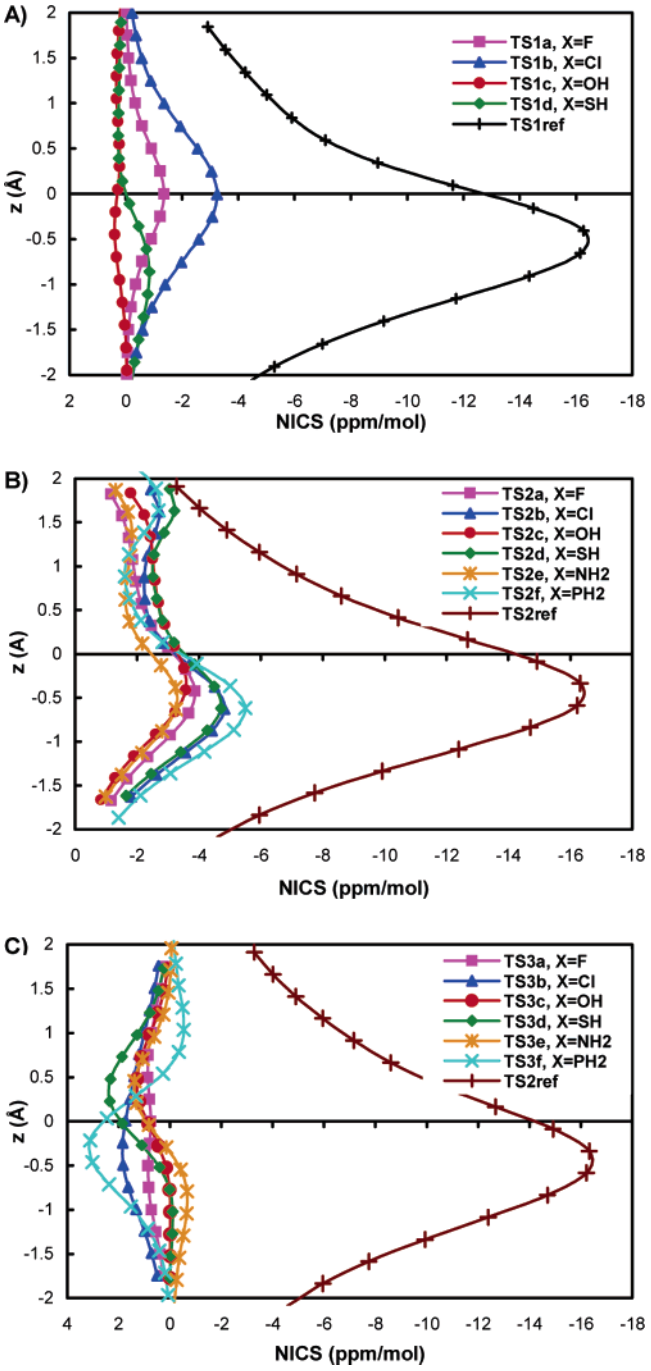


**FIGURE 8.** Plot of the calculated NICS values versus *z* for (A) transition structures **TS1a**−**d** and **TS1ref**, (B) transition structures **TS2a**−**f** and **TS2ref**, and (C) transition structures **TS3a**−**f** and again, for comparative purposes, **TS2ref**. The NICS values have been obtained at the GIAO−B3LYP/6-31+G*//B3LYP/6-31+G* level.

Closely related to these ring closures are the electrocyclizations of dienyl ketenes to 2,4-cyclohexadienones, which have been the subject of theoretical studies by Zora,[32b,36] showing that the corresponding transition structures adopt slightly nonplanar conformations, in contrast to the boatlike conformation found for **TS2ref**. Those different geometries were ascribed to the fact that the LUMO orbital of the ketene moiety easily

(36) Zora, M.; Sahpaz, F.; Ozarslan, E. *J. Mol. Structure (THEOCHEM)* **2002**, *589*−*590*, 111−112.

**TABLE 3. NICS Values Computed at the Ring Critical Point of the Electron Density ($NICS_{RCP}$) and Maximum[a] NICS Values along the *z* Axis ($NICS_{Max}$) in ppm·mol$^{-1}$ in TS1a−d, TS2a−f, and TS3a−f Calculated at the GIAO-B3LYP/6-31+G*//B3LYP/6-31+G* Theoretical Level**

| transition structure | $NICS_{RCP}$ | $NICS_{max}$ |
|---|---|---|
| **TS1a** (X = F) | −1.36 at 0.00 Å | −1.36 at 0.00 Å |
| **TS1b** (X = Cl) | −3.24 at 0.00 Å | −3.24 at 0.00 Å |
| **TS1c** (X = OH) | +0.28 at 0.05 Å | +0.40 at −0.45 Å |
| **TS1d** (X = SH) | −0.13at −0.11 Å | −0.84 at −0.86 Å |
| **TS1ref**[b] | −14.48 at −0.16 Å | −16.27 at −0.41 Å |
| **TS2a** (X = F) | −3.01 at 0.07 Å | −3.87 at −0.43 Å |
| **TS2b** (X = Cl) | −2.86 at 0.12 Å | −4.82 at −0.63 Å |
| **TS2c** (X = OH) | −3.21 at 0.08 Å | −3.57 at −0.41 Å |
| **TS2d** (X = SH) | −3.20 at 0.13 Å | −4.71 at −0.62 Å |
| **TS2e**[c] (X = $NH_2$) | −2.17 at 0.12 Å | −3.25 at −0.63 Å |
| **TS2f** (X = $PH_2$) | −2.83 at 0.14 Å | −5.50 at −0.61 Å |
| **TS2ref**[d] | −14.92 at −0.09 Å | −16.32 at −0.34 Å |
| **TS3a** (X = F) | +0.75 at 0.00 Å | +0.87 at ± 0.5 Å |
| **TS3b** (X = Cl) | +1.73 at 0.00 Å | +1.84 at −0.24 Å |
| **TS3c** (X = OH) | +0.84 at −0.03 Å | +1.29 at 0.47 Å |
| **TS3d** (X = SH) | +1.85 at −0.02 Å | +2.34 at 0.23 Å |
| **TS3e**(X = $NH_2$) | +0.82 at −0.04 Å | +1.38 at 0.46 Å |
| **TS3f** (X = $PH_2$) | +2.46 at 0.04 Å | +3.11 at −0.21 Å |

[a] Maximum NICS value by considering absolute values. [b] Transition state corresponding to the [1,5]-H shift in 1,3-pentadiene. [c] NICS values computed at the B3LYP/6-31+G* level in **TS2e** optimized at the HF/6-31G* level. [d] Transition state corresponding to the 6$\pi$-electrocyclic ring closure of 1,3,5-hexatriene leading to 1,3-cyclohexadiene.

interacts with the terminal C═C bond without disturbing so much the planarity of the transition state. On the basis of these geometries and the NICS values computed at the center of the forming rings, Zora established the pseudopericyclic nature of the cyclization of dienyl ketenes, although, recently, this assumption has provoked some controversy.[27c] Another related cyclization, that of *o*-vinylphenylisocyanate to quinolin-2(1*H*)-one, occurring via a monorotatory transition state, has been qualified by Dolbier as pseudopericyclic.[24i]

**Transition Structures TS3a−f.** The NBO analyses show that in these transition structures the new partially formed $\sigma$C1−O12 bond results mainly from the interaction between a lone pair of the carbonylic oxygen atom (which changes from a nonbonding $sp^2$ orbital to a bonding $sp^3$ orbital) and a p orbital of the C1═N3 system, and not from the interaction between the $\pi$C6−O12 and the $\pi$C1═N3 systems expected for a transition state of pericyclic nature (see selected interactions from the second-order perturbation analyses in the Supporting Information). From the geometries of these transition structures and the NBO analyses, it can be inferred that the lone pair at the nitrogen atom N3 is changing from a nonbonding $sp^2$ orbital to a p orbital for forming part of the new $\pi$N3═C4 system, whereas the initial p orbital at the N3 atom changes to an $sp^2$ orbital accommodating the lone pair in the final oxazine. In the C6−O12 terminus, the initial p orbital at the carbonylic oxygen atom rehibridizes to an $sp^3$ orbital for accommodating a lone pair in the final oxazine. The nonaromaticity of these structures was confirmed by the low absolute values of the NICS along the *z* axis, which are depicted in Figure 8C, along with those corresponding to the transition structure **TS2ref** for comparison.

There are several reports dealing with pseudopericyclic electrocyclizations closely related to the cyclization of ketenimines **8** to the 1,3-oxazines **11**,[16,23g,24a,27b] where the pseudopericyclic nature of these processes was established on the basis of the planar geometries of the corresponding transition states or their magnetic properties.

## Conclusions

In this study a peculiar tandem sequence of two pseudopericyclic events, [1,5]-X sigmatropic shift and further 6$\pi$-electrocyclic ring closure, has been unraveled both on experimental and theoretical bases. Different X groups have been analyzed when supported on a *N*-[2-(X-carbonyl)phenyl ketenimine fragment. The relative migratory aptitude of such groups in the sigmatropic step has been determined experimentally as being RSe $\approx$ RS $\gg$ $R_2N$ $\approx$ ArO. The migrating aptitudes of the different X groups at the acyl substituent in the *N*-(2-X-carbonyl)vinyl ketenimines considered in the theoretical study is predicted to be $PH_2$ > Cl > SH > $NH_2$ > F > OH. The first step of the transformation of the *N*-(2-X-carbonyl)vinyl ketenimines into the final 2-X-4(3*H*)-pyridones, the sigmatropic shift, is always rate-determining and may occur either in a concerted or stepwise manner (via zwitterionic intermediates), depending on the nature of the migrating group X. A pseudopericyclic topology have been found for the transition states of some of the [1,5]-X migration (X = F, Cl, OH, SH), and those corresponding to the second step, the 6$\pi$-electrocyclization of the ketene intermediates to the pyridones. An alternative cyclization mode of these ketenimines, the formation of 1,3-oxazines via an initial 6$\pi$-electrocyclic ring closure, has been also considered and calculated to be of pseudopericyclic nature. The marked modal selectivity of the whole system found in the experiments (exclusive formation of quinolin-4(3*H*)-ones versus benzoxazines) could be rationalized on the basis of the calculated energy barriers for the individual steps.

## Experimental Section

**Computational Methods.** All calculations were carried out with the Gaussian98[37] and Gaussian03[38] suite of programs. An intensive characterization of the potential energy surface was done at the HF/6-31G*[39] theoretical level and then with the B3LYP[40] functional using the 6-31+G* basis set. All the reported stationary points were fully optimized by analytical gradient techniques. Harmonic frequency calculations at each level of theory verified the identity of each stationary point as a minimum or a transition state and were used to provide an estimation of the zero-point vibrational energies (ZPVE), which were not scaled. IRC calculations were carried out in order to determine what minima each transition structure connects. Second-order perturbation analyses were achieved with the NBO (natural bond orbital) method.[41] NICS values were obtained at the B3LYP/6-31+G* level with the GIAO (gauge-independent atomic orbital) method.[42]

**Preparation of 2-Arylselenoquinolin-4(3*H*)-ones 5m−o.** To a solution of the corresponding *Se*-aryl 2-azidoselenobenzoate **2** (1 mmol) in anhydrous toluene (15 mL) was added triphenylphosphine (0.26 g, 1 mmol), and the reaction mixture was stirred at room temperature for 4 h. Next, a solution of diphenylketene (0.19 g, 1 mmol) or methylphenylketene (0.13 g, 1 mmol) in anhydrous toluene (2 mL) was added. The new reaction mixture was first stirred at room temperature for 15 min and then at reflux temperature for 1 h. After cooling, the solvent was removed under reduced pressure. The resulting material was chromatographed on silica gel using hexanes/diethyl ether (7:3, v/v) as eluent.

Some of the 2-arylselenoquinolin-4(3*H*)-ones **5** prepared could not be obtained as crystalline solids. For these compounds, after removing the chromatographic solvents under reduced pressure, the resulting solids were triturated, dried at 50 °C under high vacuum for 24 h, and used as such for characterization.

**3,3-Diphenyl-2-phenylselenoquinolin-4(3*H*)-one 5m:** yield 62%; mp 182−184 °C (yellow prisms, $Et_2O$); IR (Nujol) 1683 (vs), 1599 (w), 1580 (s), 1561 (vs), 1285 (m), 1154 (w), 1119 (w), 1068 (w), 891 (w), 777 (w), 767 (m), 751 (m), 700 (s), 657 (m), 633 (s) $cm^{-1}$; $^1H$ NMR ($CDCl_3$, 300 MHz) $\delta$ 7.17−7.20 (m, 2 H), 7.35 (s, 10 H), 7.40−7.43 (m, 3 H), 7.49 (td, 1 H, $J$ = 7.6, 1.4 Hz), 7.64−7.67 (m, 2 H), 7.77 (dd, 1 H, $J$ = 7.9, 1.5 Hz); $^{13}C$ NMR ($CDCl_3$, 75 MHz) $\delta$ 72.1 (s), 121.8 (s), 126.5, 127.4, 127.7, 128.6, 128.7, 128.8, 129.0, 130.4, 135.8, 136.3, 137.5 (s), 146.2 (s), 178.9 (s), 197.1 (s); MS (EI, 70 eV) *m*/*z* (rel int) 453 ($M^+$ for $^{80}Se$, 12), 451 ($M^+$ for $^{78}Se$, 6), 296 (100). Anal. Calcd for $C_{27}H_{19}NOSe$ (452.41): C, 71.68; H, 4.23; N, 3.10. Found: C, 71.57; H, 4.24; N, 3.01.

**Preparation of 2-Aryloxyquinolin-4(3*H*)-ones 5p−s and 2-Aminoquinolin-4(3*H*)-ones 5t−v.** A solution of the corresponding 2-(triphenylphosphoranylideneamino)benzoate **3** (1 mmol) or the 2-(triphenylphosphoranylideneamino)benzamide **3** (1 mmol) in anhydrous dichloromethane (5 mL) was introduced in a glass tube, and a solution of diphenylketene (0.19 g, 1 mmol) or methylphenylketene (0.13 g, 1 mmol) in the same solvent (2 mL) was added. After stirring at room temperature for 15 min the solvent was removed to dryness under reduced pressure. The glass tube was sealed and the mixture containing the corresponding ketenimine **4** and triphenylphosphine oxide was heated at 230 °C for 1 h. After cooling at room temperature, the crude mixture was dissolved in dichloromethane (20 mL) and transferred to a round-bottom flask. Finally, the solvent was removed under reduced pressure and the resulting material was chromatographed on a silica gel column using hexanes/diethyl ether as eluent.

Some of the 2-aryloxyquinolin-4(3*H*)-ones and 2-aminoquinolin-4(3*H*)-ones **5** prepared could not be obtained as crystalline solids.

(37) Frisch, M. J.; Trucks, G. W.; Schlegel, H. B.; Scuseria, G. E.; Robb, M. A.; Cheeseman, J. R.; Zakrzewski, V. G.; Montgomery, J. A., Jr.; Stratmann, R. E.; Burant, J. C.; Dapprich, S.; Millam, J. M.; Daniels, A. D.; Kudin, K. N.; Strain, M. C.; Farkas, O.; Tomasi, J.; Barone, V.; Cossi, M.; Cammi, R.; Mennucci, B.; Pomelli, C.; Adamo, C.; Clifford, S.; Ochterski, J.; Petersson, G. A.; Ayala, P. Y.; Cui, Q.; Morokuma, K.; Malick, D. K.; Rabuck, A. D.; Raghavachari, K.; Foresman, J. B.; Cioslowski, J.; Ortiz, J. V.; Baboul, A. G.; Stefanov, B. B.; Liu, G.; Liashenko, A.; Piskorz, P.; Komaromi, I.; Gomperts, R.; Martin, R. L.; Fox, D. J.; Keith, T.; Al-Laham, M. A.; Peng, C. Y.; Nanayakkara, A.; Gonzalez, C.; Challacombe, M.; Gill, P. M. W.; Johnson, B.; Chen, W.; Wong, M. W.; Andres, J. L.; Gonzalez, C.; Head-Gordon, M.; Replogle, E. S.; Pople, J. A. *Gaussian 98*, Revision A.9; Gaussian, Inc.: Pittsburgh, PA, 1998.

(38) Frisch, M. J.; Trucks, G. W.; Schlegel, H. B.; Scuseria, G. E.; Robb, M. A.; Cheeseman, J. R.; Montgomery, J. A.; Vreven, T.; Kudin, K. N.; Burant, J. C.; Millam, J. M.; Iyengar, S. S.; Tomasi, J.; Barone, V.; Mennucci, B.; Cossi, M.; Scalmani, G.; Rega, N.; Petersson, G. A.; Nakatsuji, H.; Hada, M.; Ehara, M.; Toyota, K.; Fukuda, R.; Hasegawa, J.; Ishida, M.; Nakajima, T.; Honda, Y.; Kitao, O.; Nakai, H.; Klene, M.; Li, X.; Knox, J. E.; Hratchian, H. P.; Cross, J. B.; Adamo, C.; Jaramillo, J.; Gomperts, R.; Stratmann, R. E.; Yazyev, O.; Austin, A. J.; Cammi, R.; Pomelli, C.; Ochterski, J. W.; Ayala, P. Y.; Morokuma, K.; Voth, G. A.; Salvador, P.; Dannenberg, J. J.; Zakrzewski, V. G.; Dapprich, S.; Daniels, A. D.; Strain, M. C.; Farkas, O.; Malick, D. K.; Rabuck, A. D.; Raghavachari, K.; Foresman, J. B.; Ortiz, J. V.; Cui, Q.; Baboul, A. G.; Clifford, S.; Cioslowski, J.; Stefanov, B. B.; Liu, G.; Liashenko, A.: Piskorz, P.; Komaromi, L.; Martin, R. L.; Fox, D. J.; Keith, T.; Al-Laham, M. A.; Peng, C. Y.; Nanayakkara, A.; Challacombe, M. P.; Gill, M. W.; Johnson, B. G.; Chen, W.; Wong, M. W.; Gonzalez, C.; Pople, J. A. *Gaussian 03*, Revision B.03; Gaussian, Inc.: Pittsburgh, PA, 2003.

(39) Hehre, W. J.; Radom, L.; Schleyer, P. v. R.; Pople, J. A. In *Ab Initio Molecular Orbital Theory*; Wiley: New York, 1986, pp 71−82, and references therein.

(40) (a) Parr, R. G.; Yang, W. *Density-Functional Theory of Atoms and Molecules*; Oxford University Press: New York, 1989. (b) Bartolotti, L. J.; Fluchichk, K. In *Reviews in Computational Chemistry*; Lipkowitz, K. B., Boyds, D. B., Eds.; VCH Publishers: New York, 1996; Vol. 7; pp 187−216. (c) Kohn, W.; Becke, A. D.; Parr, R. G. *J. Phys. Chem*. **1996**, *100*, 12974−12980. (d) Ziegler, T. *Chem. Rev*. **1991**, *91*, 651−667.

(41) (a) Redd, A. E.; Weinstock, R. B.; Weinhold, F. *J. Chem. Phys*. **1985**, *83*, 735−746. (b) Reed, A. E.; Curtiss, L. A.; Weinhold, F. *Chem. Rev*. **1988**, *88*, 899−926. (c) Reed, A. E.; Schleyer, P. v. R. *J. Am. Chem. Soc*. **1990**, *112*, 1434−1445.

(42) Wolinski, K.; Hilton, J. F.; Pulay, P. *J. Am. Chem. Soc*. **1990**, *112*, 8251−8260.

For these compounds, after removing the chromatographic solvents under reduced pressure, the resulting solids were triturated, dried at 50 °C under high vacuum for 24 h, and used as such for characterization.

**2-(4-Methylphenyloxy)-3,3-diphenylquinolin-4(3*H*)-one 5p:** column chromatography, hexanes/diethyl ether (4:1, v/v); yield 42%; mp 201−202 °C (yellow prisms, $Et_2O$); IR (Nujol) 1682 (vs), 1641 (vs), 1598 (vs), 1504 (vs), 1268 (vs), 1244 (vs), 1197 (vs), 1013 (m), 861 (w), 761 (s), 702 (s) $cm^{-1}$; $^1H$ NMR ($CDCl_3$, 300 MHz) $\delta$ 2.32 (s, 3 H), 6.93 (d, 2 H, $J$ = 8.3 Hz), 7.13 (d, 2 H, $J$ = 8.3 Hz), 7.21 (t, 1 H, $J$ = 7.4 Hz), 7.26 (d, 1 H, $J$ = 8.1 Hz), 7.30−7.36 (m, 10 H), 7.52 (td, 1 H, $J$ = 8.1, 1.5 Hz), 7.95 (d, 1 H, $J$ = 7.7 Hz); $^{13}C$ NMR ($CDCl_3$, 75 MHz) $\delta$ 20.9, 67.1 (s), 121.4, 122.1 (s), 126.5, 127.3, 127.5, 128.0, 128.5, 129.6, 129.7, 135.0 (s), 136.2, 138.9 (s), 146.6 (s), 150.2 (s), 168.5 (s), 196.7 (s); MS (EI, 70 eV) *m*/*z* (rel int) 403 ($M^+$, 25), 77 (100). Anal. Calcd for $C_{28}H_{21}NO_2$ (403.48): C, 83.35; H, 5.25; N, 3.47. Found: C, 83.18; H, 5.27; N, 3.32.

**2-(*N*,*N*-Dimethyl)amino-3,3-diphenylquinolin-4(3*H*)-one 5t:** column chromatography, hexanes/diethyl ether (2:3, v/v); yield 36%; mp 242−244 °C (yellow prisms, $Et_2O$); IR (Nujol) 1670 (s), 1599 (m), 1544 (vs), 1492 (m), 1393 (s), 1292 (m), 1269 (m), 1217 (w), 1177 (m), 1142 (m), 999 (w), 871 (w), 763 (m), 742 (w), 696 (m) $cm^{-1}$; $^1H$ NMR ($CDCl_3$, 400 MHz) $\delta$ 2.80 (s, 6 H), 6.90 (t, 1 H, $J$ = 7.4 Hz), 7.23−7.25 (m, 1 H), 7.27−7.35 (m, 6 H), 7.43−7.47 (m, 5 H), 7.67 (dd, 1 H, $J$ = 7.8, 1.3 Hz); $^{13}C$ NMR ($CDCl_3$, 100 MHz) $\delta$ 40.0, 66.1 (s), 118.6 (s), 122.6, 125.9, 127.2, 127.8, 128.7, 129.2, 136.3, 137.4 (s), 151.4 (s), 166.3 (s), 196.9 (s); MS (EI, 70 eV) *m*/*z* (rel int) 340 ($M^+$, 100). Anal. Calcd for $C_{23}H_{20}N_2O$ (340.42): C, 81.15; H, 5.92; N, 8.23. Found: C, 81.01; H, 5.77; N, 8.34.

**Acknowledgment.** We are grateful to the "Ministerio de Educación y Ciencia" of Spain and FEDER (Project CTQ2005-02323/BQU) and the "Fundación Séneca-CARM" (Project PI-1/00749/FS/01) for funding. M.-M.O. thanks Fundación Cajamurcia for a fellowship.

**Supporting Information Available:** Experimental details for the synthesis of compounds **2k**−**q**, **3k**−**q**, and **4a** and their characterization (NMR, IR, MS, elemental analyses); spectroscopic data for compounds **5n**−**o**, **5q**−**s**, and **5u**,**v**; Table S1, including the chief electronic and energetic features for all stationary points discussed in the text; Cartesian coordinates of local minima and transition structures discussed in the text; Table S2, including selected interaction from the second-order perturbation theory analysis of **TS1a**−**d**, **TS2a**−**f**, and **TS3a**−**f**; Figures S1−S3, showing the B3LYP/6-31+G*-optimized geometries of **TS1a**−**d**, **TS1ref**, **TS2a**−**f**, **TS2ref**, and **TS3a**−**f** and the points used to evaluate the NICS. This material is available free of charge via the Internet at http://pubs.acs.org.

JO061286E